Species Selection Regime and Phylogenetic Tree Shape

G. Anthony Verboom[1,*], Florian C. Boucher[2,3], David D. Ackerly[4,5], Lara M. Wootton[1], and
William A. Freyman[4,6]

[1]*Bolus Herbarium and Department of Biological Sciences, University of Cape Town, Private Bag, Rondebosch 7700, South Africa;* [2]*Department of Botany
and Zoology, University of Stellenbosch, Private Bag X1, Matieland 7602, South Africa;* [3]*Université Grenoble Alpes, CNRS, Laboratoire d'Ecologie Alpine
(LECA), 2233 Rue de la Piscine, FR-38000 Grenoble, France;* [4]*Department of Integrative Biology, University of California, Berkeley, CA 94720, USA;*
[5]*Department of Environmental Sciences, Policy, and Management, University of California, Berkeley, CA 94720, USA; and* [6]*Department of Ecology,
Evolution and Behavior, University of Minnesota, Saint Paul, MN 55108, USA*
*Correspondence to be sent to: Bolus Herbarium and Department of Biological Sciences, University of Cape Town, Private Bag, Rondebosch 7700, South
Africa;*
E-mail: tony.verboom@uct.ac.za

Abstract.—Species selection, the effect of heritable traits in generating between-lineage diversification rate differences, provides a valuable conceptual framework for understanding the relationship between traits, diversification, and phylogenetic tree shape. An important challenge, however, is that the nature of real diversification landscapes—curves or surfaces which describe the propensity of species-level lineages to diversify as a function of one or more traits—remains poorly understood. Here, we present a novel, time-stratified extension of the QuaSSE model in which speciation/extinction rate is specified as a static or temporally shifting Gaussian or skewed-Gaussian function of the diversification trait. We then use simulations to show that the generally imbalanced nature of real phylogenetic trees, as well as their generally greater than expected frequency of deep branching events, are typical outcomes when diversification is treated as a dynamic, trait-dependent process. Focusing on four basic models (Gaussian-speciation with and without background extinction; skewed-speciation; Gaussian-extinction), we also show that particular features of the species selection regime produce distinct tree shape signatures and that, consequently, a combination of tree shape metrics has the potential to reveal the species selection regime under which a particular lineage diversified. We evaluate this idea empirically by comparing the phylogenetic trees of plant lineages diversifying within climatically and geologically stable environments of the Greater Cape Floristic Region, with those of lineages diversifying in environments that have experienced major change through the Late Miocene-Pliocene. Consistent with our expectations, the trees of lineages diversifying in a dynamic context are less balanced, show a greater concentration of branching events close to the present, and display stronger diversification rate-trait correlations. We suggest that species selection plays an important role in shaping phylogenetic trees but recognize the need for an explicit probabilistic framework within which to assess the likelihoods of alternative diversification scenarios as explanations of a particular tree shape. [Cape flora; diversification landscape; environmental change; gamma statistic; species selection; time-stratified QuaSSE model; trait-dependent diversification; tree imbalance.]

The concept of species selection, first introduced by Stanley (1975) and refined by others (e.g., Eldredge and Cracraft 1980; Vrba 1984; Coyne and Orr 2004; Jablonski 2008), provides a conceptual framework for understanding the relationship between traits, diversification, and phylogenetic tree shape. As appreciated by Rabosky and McCune (2009), "questions about variation in diversification rates among clades are fundamentally questions about species selection and the broader role of process in generating biodiversity." In the broadest sense, species selection refers to the effect of heritable traits and their environmental interactions in generating differences in net diversification rate (*NDR*) among lineages. As such, it is the macroevolutionary analog of individual-level natural selection, the critical difference being that, where natural selection is powered by trait-dependent differences in individual-level fitness, species selection is powered by trait-dependent species-level differences in diversification propensity. While Vrba (1984) was at pains to distinguish strict-sense species selection, in which diversification rate differences are modulated by emergent species-level properties (e.g., range size), from "effect-macroevolution," in which interspecific variation in diversification rate is a product of selection operating at the level of individual organisms and modulated by individual-level variation (i.e., natural selection), many authors prefer to apply the concept in the broader sense (reviewed in Jablonski (2008); see also Chevin (2016)) and we follow that approach here.

In the same way that trait-based fitness landscapes (i.e., adaptive landscapes; Wright 1931, 1932; Simpson 1944) define evolutionary dynamics at the population level, "diversification landscapes"—curves or surfaces which describe the propensity of species-level lineages to diversify as a function of one or more traits—define the diversification dynamics of clades, and the shapes of the phylogenetic trees that they generate. The alternative states of "key innovation" traits, for example, are causally linked to differences in diversification rate (Heard and Hauser 1995), and such traits are expected to generate imbalanced phylogenetic trees (Slowinski and Guyer 1993; Chan and Moore 2002). Accordingly, heterogeneous, trait-dependent processes have repeatedly been shown to explain empirical tree shapes better than constant-rate birth–death processes (FitzJohn 2010, 2012a; Goldberg et al. 2010; Johnson et al. 2011; Freyman and Höhna 2019). While key

innovations have typically been conceptualized as discrete and evaluable using methods such as BiSSE and MuSSE (Maddison et al. 2007; FitzJohn et al. 2009; FitzJohn 2012a), the realization that continuously varying traits must also influence diversification has led to the development of quantitative trait-dependent diversification models (QuaSSE; FitzJohn 2010). An important challenge of such methods, however, is that the nature of empirical diversification landscapes has received little attention and remains poorly understood (Freckleton et al. 2008; FitzJohn 2010). This stands in marked contrast to the situation for natural selection, where the form of the fitness landscape is encapsulated in terms such as stabilizing, directional and disruptive selection and where the role of trait–trait fitness interactions in producing multimodal fitness landscapes (Wright 1932) is widely appreciated (e.g., Arnold et al. 2001, Ridley 2003). Thus, while QuaSSE implements a number of alternative diversification functions to describe different diversification landscapes (i.e., constant, Gaussian, sigmoidal, linear), the biological underpinnings of these models are sometimes unclear. It is widely recognized, for example, that empirical phylogenetic trees tend to be less balanced than those obtained under a constant diversification function (e.g., Guyer and Slowinski 1993; Heard 1996; Blum and François 2006; Stadler et al. 2016). In addition, the fact that the constant, sigmoidal and linear functions ascribe non-zero diversification rates to extreme (including infinitely large or small) values of the diversification trait seems unrealistic given the bounded nature of variation in most biological traits; for example, seed size (Westoby et al. 1992) and leaf size (Parkhurst and Loucks 1972; Jensen and Zwieniecki 2013).

The aim of this article, then, is to explore the impacts of historical species selection on tree shape, including both clade balance and branching time distribution, and on the relationship of diversification rate to values of the underlying "diversification trait" (i.e., the trait determining diversification). First, we use model-based simulations to understand better the manner in which different species selection regimes influence tree shape. Then, using a synthesis of our simulation results as an interpretive guide, we compare the shapes of empirical phylogenies evolving under contrasting species selection regimes.

In our simulations, we focus on the Gaussian diversification function included in QuaSSE because the boundedness of this function, in our view, renders it more realistic than unbounded-trait models. Moreover, the only existing study which to our knowledge compares the fits of alternative diversification functions to an empirical data set finds that diversification in New World rattlesnakes is best described as a Gaussian function of a multivariate ecological niche axis (Pyron and Burbrink 2012). Where diversification in this example is most consistent with *accelerated speciation* under intermediate values of the diversification trait, a pattern consistent with radiation in an adaptive zone (*sensu* Simpson 1953) whose ecological extent (i.e., in terms of the environmental variables that define it and the organismal traits which enable its utilization) is normally distributed, Gaussian diversification might equally arise via *reduced extinction* in morphologically average lineages (cf. Liow 2007). Accordingly, we include both Gaussian-speciation and Gaussian-extinction scenarios in our simulations. Also, since we can envisage scenarios in which diversification rate is maximized under extreme trait values, as in the case of traits such as dispersal rate, niche specificity and plant size (Jablonski 2008; Lengyel et al. 2009; Claramunt et al. 2012; Ebel et al. 2015; Boucher et al. 2017) which influence genetic differentiation directly through their effects on gene flow and/or niche partitioning, we also consider skewed-Gaussian-speciation functions in our simulations. Such skewed distributions can, of course, also be modeled adequately as a Gaussian function of log-transformed trait values (see Oliver et al. 2007).

Finally, recognizing that environmental conditions have changed over time and that this may represent a change in species selection regime, with consequences for trait-modulated diversification (e.g., Vrba 1985; Heard 1996), we examine the impacts of these diversification functions both in a static context and in a manner emulating a long-term environmental trend. For this purpose, we develop simulation functions for a novel, time-stratified extension of FitzJohn's (2010) QuaSSE model which incorporates time-dependency in the function relating speciation and/or extinction rate to a diversification trait. Long-term environmental trends are a general feature of Earth history, operating at a variety of temporal and spatial scales (e.g., Zachos et al. 2001) and have, in many cases, been thought to influence diversification and diversity patterns in a trait-modulated manner. For example, the Cretaceous radiation of angiosperms, which underpins an extreme case of phylogenetic imbalance (Darwin and Seward 1903; Sanderson and Donoghue 1994; Davies et al. 2004), has been linked to changes in global climate and/or atmospheric $[CO_2]$ which are thought to have favored angiosperms on account of their ability to simultaneously enhance assimilation capacity and water use efficiency under dropping atmospheric $[CO_2]$ (Franks and Beerling 2009; Brodribb et al. 2009; Brodribb and Field 2010).

Here, we test the general hypothesis that historical species selection underpins the tendency for real phylogenetic trees to be more imbalanced than expected under a constant-rate model and to have greater than expected frequencies of deep branching events. We predict that any non-constant (e.g., Gaussian, skewed-Gaussian) diversification function fosters diversification asymmetries and, as such, has the potential to produce trees that show greater imbalance, quantified using Colless (1982) I_c metric, than those generated under a constant diversification function (i.e., $I_c >> 0$; see Supplementary Appendix 1 available

on Dryad at http://dx.doi.org/10.5061/dryad.1sf007b, Fig. 1). In addition, we predict that a temporally shifting diversification function will tend to exaggerate imbalance by promoting, consistently over time, diversification in lineages with extreme trait values. Following Heard 1996, p. 2146), we also predict that a directionally changing species selection regime will produce a correlation ($r_{rate-trait}$) between species-specific diversification rates, quantified as the number of divergence events connecting each species to the root node (Freckleton et al. 2008), and species-specific values of the trait(s) responsible for diversification (i.e., $|r_{rate-trait}| >> 0$; see Supplementary Appendix 1 available on Dryad, Fig. 1). Finally, following Pybus and Harvey (2000), we predict that the frequency of deep branches in the tree, quantified using the gamma (γ) statistic (Pybus and Harvey 2000) depends primarily on whether extinction is a feature of the diversification process. Where this is the case, γ should be >0; where not, it should be <0 since movement toward the margins of a bounded, non-constant diversification function compromises the ability of lineages to speciate toward the present (see Supplementary Appendix 1 available on Dryad, Fig. 1).

As an empirical test of our theoretical predictions, we compare the phylogenetic tree shapes of plant lineages associating with environments in the Greater Cape Floristic Region (GCFR) of South Africa, which differ in terms of their climatic and geological stability from the Late Miocene onwards. Where the infertile, quartzitic landscapes of the Cape Fold Mountains are believed to have remained fairly unchanged geologically for much of the Cenozoic, on account of their hard rocks (Scharf et al. 2013), the more fertile, shale and granite geologies which dominate the intermontane valleys and coastal plains may have been exposed only recently, possibly as a consequence of tectonic uplift around the Miocene-Pliocene boundary (Cowling et al. 2009). In addition, where the higher elevations of the Cape Fold Mountains are characterized by a relatively wet and equable climate resembling that which prevailed in the GCFR during the Early and Middle Miocene (e.g., Linder 2003), the lower-elevation areas, particularly in the west, are today characterized by an acutely summer-arid climate whose origin can be traced to the Late Miocene (Dupont et al. 2011; Hoffmann et al. 2015). The overall conclusion is that, where the moist, quartzitic environments of the Cape mountains have enjoyed relative geological and climatic stability over the past 10 myr, the lowland and west coast areas have experienced significant climatic and geological change.

Since these two sets of environments are dominated by vegetation types (fynbos heathlands in wet, quartzitic mountain habitats; succulent and asteraceous renosterveld scrubland in summer-arid, fertile lowland habitats) which are floristically distinct at the genus and family levels (Bergh et al. 2014), it is possible to identify lineages which have diversified primarily within the context of comparative environmental stability
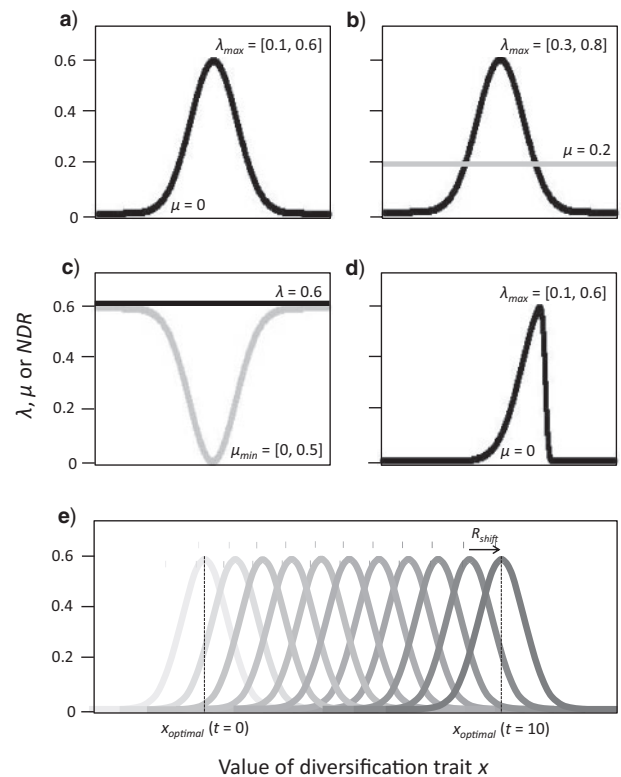

FIGURE 1. Trait-dependent diversification models employed in simulations. a) Under the "Gaussian-speciation" model with no extinction, speciation rate (λ) varies as a Gaussian function of a diversification trait (x), while extinction rate (μ) is independent of x and set to 0. The value of x is allowed to "evolve" according to a Brownian motion process with a diffusion parameter β, and the maximum speciation rate (λ_{max} = [0.1, 0.6]) is associated with the mean of the Gaussian function $f(x)$ whose variance (σ_x^2) was set to 0.1 in our simulations. b) Under the "Gaussian-extinction" model, μ varies as an "upside-down" Gaussian function of x while λ is independent of x and set to 0.6. The minimum extinction rate (μ_{min} = [0, 0.5]) is associated with the mean of the function $f(x)$. c) Under the "skewed-speciation" model λ varies as a skewed-Gaussian function of x whose skewness parameter (α) was set to 10 or -10 in our simulations. Extinction is independent of x and set to 0. d) The "Gaussian-speciation" model with random extinction is identical to the Gaussian-speciation model with zero extinction, but differs in having λ_{max} = [0.3, 0.8] and μ = 0.2. e) Finally, under shifting species selection, the diversification function moves by a set amount (i.e., R_{shift}), in a positive direction, every 1 myr. Thus, the value of x which maximizes diversification shifts over time.

(fynbos lineages) and those which have diversified under more changeable conditions (succulent and renosterveld lineages). We predict that differences in the environmental histories of such lineages will be recorded in the shapes of their phylogenetic trees. Specifically, where the long-term stability and associated low extinction rates (Dynesius and Jansson 2000; Latimer et al. 2005) associated with fynbos environments should generate trees with I_c, γ, and $r_{rate-trait}$ close to zero, the greater long-term dynamism of succulent karoo/renosterveld environments should produce trees with I_c, γ, and $|r_{rate-trait}| >> 0$.

MATERIALS AND METHODS

Simulations

As noted already, we extended FitzJohn's (2010) quantitative state speciation and extinction (QuaSSE) model to incorporate time-dependency in the simulation function that relates a quantitative diversification trait x to the diversification rates of the birth–death process. In our time-stratified QuaSSE model, each epoch or time interval k is assigned a separate function $f_k(x)$ that relates the speciation (λ_k) and extinction (μ_k) rates to the value of x during time interval k. Time-stratified phylogenetic models have been widely used to model biogeographic processes (Ree and Smith 2008; Landis 2017) but have not hitherto been applied within a state-dependent speciation and extinction framework. By keeping $f_k(x)$ constant for all time intervals we can simulate trees and traits evolving under a static species selection regime and the time-stratified model then collapses into a standard QuaSSE model. Alternatively, by defining $f_k(x)$ to be different in each of the k time intervals we can simulate diversification and trait evolution within a dynamic diversification landscape in which the species selection regime changes with time. The diversification trait x itself evolves randomly (Brownian motion) and independently along the branch segments generated by the birth–death process, potentially generating asymmetries in diversification rate across the nodes of the tree.

For the simulations presented in this study, $f_k(x)$ was specified in three ways. Under the "Gaussian-speciation" model, μ is independent of x but λ_k varies as a Gaussian function of x with a maximum speciation rate λ_{max} (Fig. 1a). Specifically,

$$f_k(x) = \lambda_{max} e^{\frac{1}{2}\left(\frac{x-\mu_k}{\sigma}\right)^2}.$$

This model was applied both in the absence (Fig. 1a) and presence of random background extinction (Fig. 1b). In contrast, under the "Gaussian-extinction model," λ_k is independent of x but μ_k varies as an "upside-down" Gaussian function of x whose optimum corresponds to a minimum extinction rate μ_{min} (Fig. 1c). In this model, λ is constant and positive, with $\mu_k \approx \lambda$ for x far from the optimum and $\mu_k < \lambda$ for x close to the optimum. Thus, while NDR varies as a Gaussian function of x under both the Gaussian-speciation and Gaussian-extinction models, in the first, NDR_{max} is a consequence of increased speciation (i.e., $\lambda_{max} - \mu$) and in the second it is a consequence of reduced extinction (i.e., $\lambda - \mu_{min}$). Finally, under the "skewed-speciation" model, μ is independent of x but λ_k varies as a skewed-Gaussian function of x with a maximum speciation rate λ_{max} (Fig. 1d). In this case, the location of the λ_{max} relative to the bounds of the distribution is defined by the skewness parameter α, with the skewed-Gaussian function reducing to a normal Gaussian function when $\alpha = 0$. For the purpose of our simulations, we set $\alpha = 10$ or -10, which locates the λ_{max} near the lower or upper

bound, respectively (Fig. 1c: $\alpha = -10$). We did not explore the effects of a skewed-extinction model.

We ran two simulation experiments. The first was designed to assess how different species selection regimes, as specified by the Gaussian-speciation, Gaussian-extinction, and skewed-speciation functions, influence tree shape, where each species selection regime is held constant over time. For this comparison, we used as a control a model in which diversification is trait-independent (i.e., constant model). For all models, simulations were done for NDR or NDR_{max} in the range [0.1, 0.6]. In the case of the Gaussian- and skewed-speciation models, μ was set to 0 and λ_{max} to [0.1, 0.6], while for the Gaussian-extinction model, λ and baseline μ were both set to 0.6, with the "upside-down" extinction function specifying μ_{min} in the range [0, 0.5]. In addition to the above, the Gaussian-speciation model was also run with $\mu = 0.2$ and λ_{max} to [0.3, 0.8] in order to assess the effects of background random extinction on pattern. Since the diffusion parameter (β) of the diversification trait x determines whether and how quickly a lineage is able to reach the bounds of a diversification function, whose variance (σ_x^2) in this study was fixed arbitrarily at 0.1, the static peak simulations were run using values of β in the range [0.005, 5.0] which matches a range of empirical estimates ($\beta = 0.007 - 2.08$; Ackerly 2009).

One hundred replicate simulations were run for each combination of λ or λ_{max}, μ or μ_{min} and β, each simulation being run over 10 myr, and initiating with $x = 0$ and a cladogenetic event on the root node. For each completed replicate, both the actual and reconstructed (i.e., excluding extinct lineages) trees were recorded, as were the values of the diversification trait at each internal and terminal node. For those parameter combinations in which ≥ 10 replicate simulations gave rise to two or more species, the following were determined: 1) the mean tree size (N; the number of "extant" species); 2) the mean tree imbalance, quantified using the Yule-normalized Colless (1982) index (I_c); 3) the mean gamma (γ) statistic (Pybus and Harvey 2000); and 4) the mean correlation ($r_{rate-trait}$) of the terminal diversification trait values with the number of internal nodes separating each terminal from the root (cf. Freckleton et al. 2008).

A second simulation experiment was used to test the effect of a temporally changing species selection regime on tree shape. For this purpose, we made use of the same diversification functions as before (with both positively and negatively skewed versions of the skewed-speciation function), but these were now shifted in a positive direction (i.e., toward larger positive values of x) every 1 myr during the course of the 10 myr simulation run (Fig. 1e). Since β and the shift rate of the diversification function (R_{shift}; determined as the magnitude of the shift at the start of each 1 myr interval) jointly determine the ability of a lineage to track the changing species-selective conditions, simulations were run for a range of values of both these parameters ($\beta = [0.005, 5.0]$; $R_{shift} = [0, 1.0]$). NDR was set to [0.2, 0.4, 0.6] and, except in the case of Gaussian-speciation, for which the effects of both $\mu = 0$

and $\mu = 0.2$ were evaluated, μ was set to 0. As in the first experiment, one hundred replicate simulations were run for each parameter combination, and the same outputs reported as before.

The determinants of variation in mean I_c, γ, and $r_{rate-trait}$ under static species selection were evaluated using linear models. To assess the impact of random extinction ($\mu = 0$ or 0.2), which was done only for Gaussian-speciation, these took the form: response variable $\sim NDR * \beta * \mu$. To assess the impact of diversification model (Gaussian-speciation, skewed-speciation, Gaussian-extinction), however, they took the form: response variable $\sim NDR * \beta *$ model. Models were simplified using backward stepwise regression, excluding first non-significant interactions and thereafter non-significant main effects, as suggested by Crawley (2007). In addition, one-sample t-tests were used to assess, for each diversification function, β and μ (the last only in the case of Gaussian-speciation), whether the mean I_c, γ, and $r_{rate-trait}$ (across all NDR) differed significantly from zero.

For the purpose of interrogating the factors influencing tree shape under shifting diversification, we focused on trees generated under $NDR = 0.6$ which showed the clearest trends. This was necessary because R_{shift} elicited complicated, nonlinear responses in all three response variables (i.e., mean I_c, γ, and $r_{rate-trait}$). Since the response curves obtained under Gaussian-speciation comprised a series of linear phases (see Results section), these responses were first decomposed using breakpoint regression analysis, with the Davies (2002) test providing an assessment of breakpoint significance. Thereafter, the determinants of I_c, γ, and $r_{rate-trait}$ were determined for the initial, pattern-generating phase using linear models of the form: response variable $\sim R_{shift} * \beta * \mu$. Comparable models were not produced for the other diversification functions (i.e., skewed-speciation and Gaussian-extinction) because the initial phase was less apparent.

Finally, to assess the extent to which trees generated under contrasting species selection regimes differ in shape we used linear discriminant analysis (LDA), applied to I_c, γ, and $r_{rate-trait}$ scores, to visualize trees obtained under the five diversification functions. For this purpose, we examined all trees with ≥ 20 species generated by the second simulation experiment under negatively skewed ($N = 762$) and positively skewed-speciation ($N = 479$), and 1000 trees with ≥ 20 species selected randomly from each of the tree sets generated under Gaussian-speciation with $\mu = 0$ and $\mu = 0.2$, and under Gaussian-extinction. Since I_c, γ, and $r_{rate-trait}$ are influenced by R_{shift}, separate LDAs were done for $R_{shift} < 0.05$, $0.05 < R_{shift} < 0.15$, $0.15 < R_{shift} < 0.25$, and $R_{shift} > 0.25$. In addition, Box and Whisker plots and one-way analysis of variance (ANOVA) were used to compare the I_c, γ, and $r_{rate-trait}$ scores of trees obtained under each diversification function.

All simulations were run in R version 3.3.1 (R Core Team 2016) making extensive use of functions included in the packages *ape* version 3.5 (Paradis et al. 2004), *diversitree* version 0.9-10 (FitzJohn 2012b), *phytools* version 0.5-38 (Revell 2012), *picante* version 1.6-2 (Kembel et al. 2010), and *geiger* version 2.0.6 (Harmon et al. 2008). Statistical analyses were also run in R, with breakpoint regressions done using the package *segmented* version 0.5-4.0 (Muggeo 2003, Muggeo 2008). Code for the time-stratified QuaSSE model and for replicating our simulations can be found in the code repository: https://github.com/wf8/species_selection_tree_shape.

Empirical Comparison

For the purpose of comparing phylogenetic tree shape between plant lineages that diversified in historically stable fynbos environments and those that diversified in climatically or geologically changeable succulent karoo or renosterveld environments we assembled a set of 14 published plant phylogenies (Table 1) meeting the following criteria:

1. Diversification centered in the GCFR of South Africa and originating from a GCFR-optimized ancestor.

2. Sampling completeness of GCFR species >65%. To assess sampling completeness we used, as a baseline, the species lists presented in Manning and Goldblatt (2012) and Snijman (2013). For consistency, infraspecific taxa were ignored throughout.

3. Dated molecular phylogeny publicly available, in electronic format.

4. Root node >10 Ma. Since succulent karoo and renosterveld landscapes were transformed by climatic and geological events taking place probably 5–8 Ma, these events would not be sufficiently well recorded in the trees of lineages originating after about 10 Ma (e.g., *Babiana*; Schnitzler et al. 2011).

Since we were explicitly interested in the impacts of within-GCFR environmental history on tree shape, the phylogenetic tree of each sampled lineage was pruned to include only species arising from the primary GCFR-centered radiation of the lineage. Thus, both non-GCFR species as well as GCFR species secondarily derived from non-GCFR lineages were removed. Also, where a species was represented by multiple accessions, all but one of these was removed, the retained accession being randomly selected.

Relying on descriptive accounts (Table 1), each species was then coded in terms of its natural occurrence (presence/absence) in fynbos, renosterveld, and succulent karoo vegetation, as defined by Bergh et al. (2014). Based on this coding, each species was assigned a "fynbos-association score" characterizing it as occurring exclusively in fynbos (1), exclusively in succulent karoo

TABLE 1. Details of dated phylogenetic trees sampled in the empirical comparison of tree shape in plant lineages radiating in the Greater Cape Floristic Region

Clade	Family	Tree size (spp)	Crown age (Ma)	Species sampling (%)	Fynbos-association score	Colless imbalance (I_c)	Gamma statistic (γ)	Tree source	Vegetation type source	Digital locality data?
Arctotidinae	Asteraceae	49	23.2	82	0.44	3.76	2.20	Hoffmann et al (2015)	None	Yes
Corycium -Pterygodium	Orchidaceae	27	18.8	84	0.61	0.63	1.25	Hoffmann et al. (2015)	Linder and Kurzweil (1999), Liltved and Johnson (2012)	Yes
Disa	Orchidaceae	75	19.4	74	0.95	1.43	−3.06	Bytebier et al. (2010)	Linder and Kurzweil (1999), Liltved and Johnson (2012)	No
Ehrharta	Poaceae	19	13.3	86	0.39	2.01	1.66	Hoffmann et al. (2015)	Fish et al. (2015); GAV pers. obs.	Yes
Elegia-Thamno -chortus	Restionaceae	99	28.3	97	0.99	0.24	0.50	Hoffmann et al. (2015)	Linder (2006)	Yes
Gladiolus	Iridaceae	89	14.1	81	0.62	3.49	3.44	Valente et al. (2011)	Goldblatt and Manning (1998)	No
Leucadendron	Proteaceae	60	21	72	0.92	0.27	0.51	Hoffmann et al. (2015)	Williams (1972), Rebelo (2001)	Yes
Moraea	Iridaceae	134	16.1	83	0.38	8.32	−1.52	Schnitzler et al. (2011)	Goldblatt (1979), 1981, 1986	Yes
Muraltia	Polygalaceae	71	10.9	64	0.73	3.71	−0.62	Verboom et al. (2009)	Levyns (1954)	No
Pentameris	Poaceae	59	14.5	92	0.80	3.09	−2.99	Hoffmann et al. (2015)	Linder (1991), Fish et al. (2015); GAV pers. obs.	Yes
Podalyrieae	Fabaceae	98	28.6	83	0.90	1.59	−1.98	Schnitzler et al. (2011)	Schutte (1997a,b), Schutte and van Wyk (2011)	No
Protea	Proteaceae	71	18.3	100	0.92	2.13	−4.15	Schnitzler et al. (2011)	Rourke (1980), Rebelo (2001)	Yes
Satyrium	Orchidaceae	24	19.6	86	0.83	1.19	−0.34	Hoffmann et al. (2015)	Linder and Kurzweil (1999), Liltved and Johnson (2012)	Yes
Tetraria	Cyperaceae	21	16.7	88	1.00	−0.50	−3.53	Slingsby et al. (2014)	GAV, pers. obs.	Yes

Notes: Species sampling is the percentage of species included relative to the full set of species listed as native to the GCFR (Manning and Goldblatt 2012; Snijman 2013). The publication from which each tree was sourced is indicated in the third column, while specialist publications used to characterize species' vegetation associations are indicated in the penultimate column. Characterization of vegetation associations also made use of Manning and Goldblatt (2012), Snijman et al. (2013), and the Red List of South African plants (http://redlist.sanbi.org/).

or renosterveld (0), or in both of these vegetation classes (0.5). For each lineage, the fynbos-association scores of individual species were then averaged to obtain a fynbos-association score for the lineage as a whole. The significance of this variable as a predictor of phylogenetic tree shape variation was then assessed by regressing the I_c and γ of each lineage's phylogenetic tree against its fynbos-association score.

Finally, recognizing the potential role of increasing seasonal aridity as a driver of diversification in the succulent karoo and renosterveld floras we assessed whether species-specific diversification rates are correlated ([Freckleton et al. 2008](#)) with species-level variation in habitat seasonality (i.e., $r_{rate-trait}$) and whether this is more pronounced in succulent karoo/renosterveld-associated lineages than in fynbos-associated lineages. For this purpose, we first characterized each species in terms of its mean precipitation seasonality (mean coefficient of variation in monthly precipitation) and its mean summer precipitation amount (mean amount of precipitation in the driest quarter). Then, having determined the $r_{rate-trait}$ of each lineage for each of these variables, we regressed the $r_{rate-trait}$ values of the various lineages against their fynbos-association scores. Species were characterized climatically using GIS functions included in the *raster* package version 2.6-7 ([Hijmans 2016](#)) for R. Since sufficiently precise (i.e., > 2000 m precision) digital locality data, based on specimens lodged in regional herbaria, were available for only 10 of the 14 lineages surveyed (Table [1](#); data sourced from [Hoffmann et al. (2015)](#) and [Verboom et al. (2015)](#)) this analysis was, of necessity, restricted to this subset of lineages.

RESULTS

Simulations

As predicted by theory, the mean I_c of trees generated under a constant diversification function with $\mu = 0$ (i.e., Yule process) does not differ significantly from 0 (Supplementary Appendix 1 available on Dryad, Fig. [2](#); $t = 0.561$, $P = 0.587$). In contrast, trees generated under static Gaussian- and skewed-speciation functions with $\mu = 0$ have mean $I_c > 0$ (Fig. 2; $t = 5.931$ to 50.818, $P < 0.001$) for all values of the Brownian diffusion parameter, β. Also, with the sole exception of trees generated under $\beta = 0.005$ ($t = 1.849$, $P > 0.05$), a static "upside-down" Gaussian-extinction function produced trees with mean $I_c > 0$ (Fig. 2; $t = 2.884$ to 5.930, $P = 0.016$ to < 0.001). In the absence of extinction, mean I_c increases linearly with *NDR*, but this relationship is dependent on both diversification function and β (Table [2a](#)). Specifically, for trees generated under a Gaussian-speciation function, mean I_c increases linearly with *NDR* under $\beta = 0.05$, 0.1, and 0.5 but not under other values of β. The reason for this is that intermediate β (i.e., $\beta = 0.05$, 0.1, and 0.5) enables some lineages to move toward the

margins of the diversification function while others remain near the peak, thereby setting up diversification asymmetries. Under $\beta < 0.05$, in contrast, imbalance is negligible because all lineages remain near the peak, and under $\beta > 0.5$ it is negligible because many lineages move to the margins. For trees generated under skewed-speciation, however, a positive relationship between *NDR* and β is apparent only at low β (i.e., $\beta = 0.005$ or 0.01; Fig. 2). This is because the density distribution described by this function is much narrower than that associated with the Gaussian-speciation function (Fig. 1a,c). Although the introduction of random background extinction ($\mu = 0.2$) weakens the relationship of mean I_c to *NDR* for trees generated under Gaussian-speciation, a positive association persists (Table [2b](#)) but this is only significant for $\beta = 0.05$ (Supplementary Fig. S2 available on Dryad). Even for trees generated under $\mu = 0.2$, mean I_c is significantly greater than 0 for all β ($t = 5.980$ to 14.549, $P < 0.001$) except $\beta = 5$ ($t = 6.608$, $P = 0.096$).

While a static "upside-down" Gaussian-extinction function consistently produced trees with mean $\gamma > 0$ (Fig. 2; $t = 15.323$ to 24.683, $P < 0.001$), static Gaussian- and skewed-speciation functions with $\mu = 0$ yielded trees with mean $\gamma < 0$ for all β (Fig. 2; $t = -6.552$ to -2539.257, $P < 0.001$). Both patterns represent departures from trees generated under a Yule process, in which mean γ is indistinguishable from 0 (Supplementary Appendix 1 available on Dryad, Fig. 2; $t = -1.611$, $P = 0.138$). A linear model reveals that, in the absence of extinction, mean γ is not related to *NDR* but is influenced by the shape of the diversification function and β, and the interaction of these variables (Table [2a](#)). The introduction of random background extinction ($\mu = 0.2$), however, produces a significant interaction between *NDR* and μ, with the mean γ of trees generated under $\mu = 0.2$ being positively related to *NDR* (Table [2b](#); Supplementary Appendix 1 available on Dryad, Fig. [3](#)). This effect is especially apparent under low β, which underpins both the negative relationship between mean γ and β, and a tendency for mean γ to be consistently greater than 0 only when $\beta < 0.1$ ($t = 3.285$ to 5.076, $P = 0.005 to < 0.001$; otherwise, for $\beta \geq 0.1$: $t = -2.900$ to 1.141, $P = 0.273$ to 0.964).

Mean $r_{rate-trait}$ is close to 0 for trees generated under static Gaussian- and skewed-speciation, both in the absence (Fig. 2) and presence (Gaussian-speciation only) of random background extinction (Supplementary Appendix 1 available on Dryad, Fig. 3). The same is true for trees generated under an "upside-down" Gaussian-extinction function (Fig. 2). Indeed, across all three diversification functions, mean $r_{trait-rate}$ differs significantly from 0 only in trees generated by skewed-speciation under $\beta = 0.005$ ($t = -3.653, P = 0.004$) and $\beta = 0.1$ ($t = -3.313$, $P = 0.008$) and by normal-extinction under $\beta = 0.01$ ($t = -2.441$, $P = 0.035$), and the deviations in these instances are slight (< 0.1). Although linear models identify mean $r_{rate-trait}$ as being influenced by an interaction of β, *NDR* and either diversification function (Table [1a](#)) or extinction (Table [1b](#)), these inferences
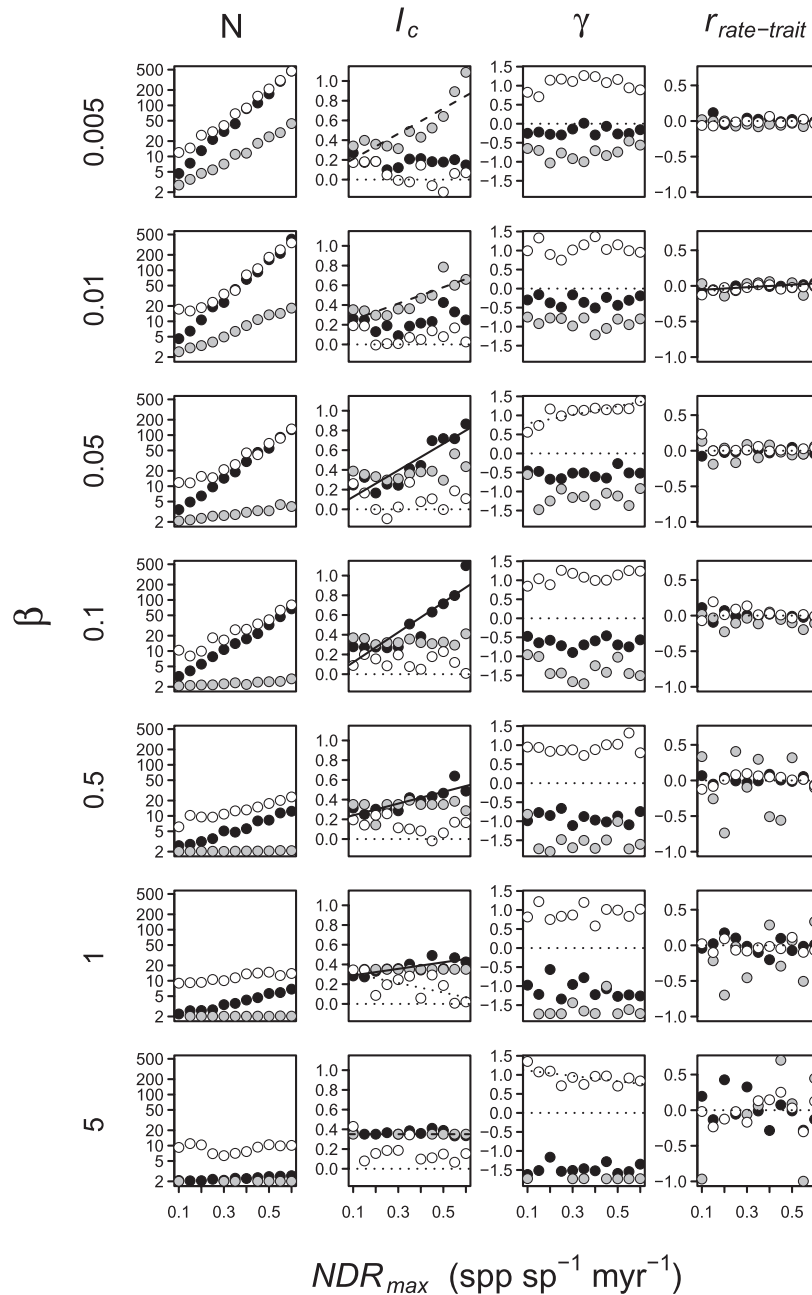
FIGURE 2.   Variation in the mean size (species number, N; log-scale), mean Yule-normalized Colless' index (I_c), mean gamma statistic (γ), and mean diversification rate-trait correlation ($r_{rate-trait}$) of trees generated under static Gaussian-speciation with $\mu = 0$ (black-filled circles), under static skewed-speciation with $\mu = 0$ (gray-filled circles), and under static Gaussian-extinction with $\lambda = 0.6$ (open circles). Results are presented for $\beta = [0.005, 5]$, and plotted against maximum net diversification rate ($NDR_{max} = \lambda_{max} - \mu$ or $\lambda - \mu_{min}$). Each point is a summary of trees generated by 100 replicate runs, excluding any runs going extinct or yielding a single species. Solid and dashed lines indicate significant bivariate relationships based on the Gaussian- and skewed-speciation data.

are misleading as they are a consequence of extreme $r_{rate-trait}$ values associated with exceptionally small (two or three species) trees generated under Gaussian- and skewed-speciation when $\beta > 0.1$.

The I_c, γ, and $r_{rate-trait}$ signatures obtained under a temporally shifting species selection regime are more complex than those obtained under static models owing to the nonlinear responses of these variables to R_{shift}

(Fig. 3). In simulations conducted in the context of a Gaussian-speciation function with $NDR = 0.6$, at least for $\beta \leq 0.1$, the relationships of mean I_c, γ and $r_{rate-trait}$ to R_{shift} reflect three linear phases which are discernible using breakpoint regression (Fig. 4; Davies test: $P < 0.05$). Starting from $R_{shift} = 0$ and with increasing R_{shift}, these describe: 1) a sharp initial increase in mean I_c and $r_{rate-trait}$, with mean γ being maintained at a high

TABLE 2. Best-fit linear models describing the responses of I_c, γ, and $r_{rate-trait}$ as functions of (a) NDR, β, and diversification model ($\mu = 0$) under a static diversification scenario; (b) NDR, μ (0 and 0.2), and β under the Gaussian-speciation model; and (c) R_{shift}, μ (0 and 0.2) and β during phase 1 ($R_{shift} < R_{crit}$; see text) of a shifting Gaussian-speciation model with high NDR (0.6)

Term	I_c	γ	$r_{rate-trait}$
(a) Static Gaussian- and skewed-speciation ($\mu = 0$), Gaussian-extinction			
Intercept	0.122**	−0.541***	−0.019
NDR	0.662***	—	—
Model (skewed-speciation)	0.124*	−0.604***	—
Model (Gaussian-extinction)	0.032	1.571***	—
β	0.038*	−0.203***	—
NDR: Model (skewed-speciation)	−0.217	—	—
NDR: Model (Gaussian-extinction)	−0.791***	—	—
NDR: β	−0.096*	—	—
Model (skewed-speciation): β	−0.019	0.058*	−0.027*
Model (Gaussian-extinction): β	0.013	0.180***	—
NDR: Model (skewed-speciation): β	—	—	−0.028*
NDR: Model (Gaussian-extinction): β	—	—	—
Model adjusted r^2	0.534***	0.930***	0.014
(b) Static Gaussian-speciation: $\mu = 0$ and 0.2			
Intercept	0.099*	−0.527***	−0.003
NDR	0.728***	—	—
μ	0.638*	3.406***	—
β	0.062*	−0.218***	0.052*
NDR: μ	−2.728***	2.788**	—
NDR: β	−0.166**	—	−0.141*
$\mu\beta$	0.284*	—	−2.082***
NDR: μ: β	—	—	3.945***
Model adjusted r^2	0.230***	0.661***	0.107***
(c) Shifting Gaussian-speciation: $R_{shift} < R_{crit}$; $\mu = 0$ and 0.2; $NDR = 0.6$			
Intercept	0.256***	−0.152***	0.055***
R_{shift}	2.908***	−0.783**	1.989***
μ	—	9.011***	—
β	7.211***	−2.315***	−0.679***
$R_{shift}\mu$	−1.871	−11.210***	−1.487***
$R_{shift}\beta$	−24.616***	—	−8.407***
μ: β	−15.895***	−46.585***	—
$R_{shift}\mu$:β	—	121.261***	—
Model adjusted r^2	0.768***	0.935***	0.875***

Notes: For (a) diversification model is a three-level factor, with Gaussian-speciation specified as the reference model. Best-fit models were determined using stepwise model simplification under the Akaike Information Criterion. Coefficients are provided only for retained terms, with significance indicated as follows: *$P < 0.05$; **$P < 0.01$; ***$P < 0.001$. Overall adjusted r^2 and significance are indicated below each model.

value; 2) a sharp decrease in all three variables; and 3) convergence of all three variables to apparent asymptotes (this phase is not apparent in all plots). The initial increase in mean I_c and $r_{rate-trait}$ (phase 1) arises because low to moderate R_{shift} promotes, consistently over time,

diversification in lineages with extreme trait values (large trait values in the case of a positive shift). Beyond some threshold R_{shift} (hereafter termed R_{crit}), however, β is insufficient to enable the diversification trait to keep abreast of the shifting diversification function, resulting in a sharp reduction in tree size and consequent declines in mean I_c, γ, and $r_{rate-trait}$ (phase 2). Consistent with this interpretation, R_{crit} is positively related to β (Supplementary Appendix 1 available on Dryad, Table 1, Fig. 4).

Focusing on phase 1 of the Gaussian-speciation simulations conducted under $\beta \leq 0.1$, a linear model confirms the dependence of both mean I_c and $r_{rate-trait}$ on R_{shift} (Table 1c), both variables attaining their maximum values around R_{crit} (Fig. 4). It also shows that these relationships are controlled by β, with higher β (i.e., $\beta = 0.05$ or 0.1) producing shallower phase 1 curves. Importantly, however, because $\beta = 0.05$ or 0.1 generates appreciable imbalance (high mean I_c) even in the absence of a shift (i.e., $R_{shift} = 0$; static Gaussian-speciation, Fig. 2), and because R_{crit} is positively related to β, the maximum imbalance generated under a Gaussian-speciation model with $\beta = 0.05$ or 0.1 (i.e., mean $I_c > 1.2$) actually exceeds that generated under lower β. Whereas the maximum imbalance achieved under $\beta = 0.005$ or 0.01 is attributable exclusively to the shape of the Gaussian-speciation function (observable in the static mode; Fig. 2), under $\beta = 0.05$ or 0.1 it is a product of both the shape of the Gaussian-speciation function and the directionally shifting nature of this function (Figs. 3 and 4). Under $\beta > 0.1$, the clearly phased relationship of mean I_c to R_{shift} disappears (Fig. 3), presumably because high β moves more lineages to the margins of the diversification function, compromising diversification rates and mean I_c. Gaussian-speciation trees consistently attain their highest γ values while $R_{shift} < R_{crit}$ (i.e., phase 1), the mean γ values of such trees being less than but close to 0 for trees generated under $\mu = 0$ and > 0 for trees generated under $\mu = 0.2$ (Supplementary Appendix 1 available on Dryad, Fig. 5). Under $R_{shift} > R_{crit}$, however, reduced diversification, associated with an inability of lineages to keep abreast of R_{shift}, produces trees which are small and in which most cladogenesis occurs before the diversification function has had a chance to shift appreciably. Such trees have lower γ, typically with mean $\gamma << 0$.

The relationships of mean I_c and γ to R_{shift} for trees generated under a skewed-speciation function differ from Gaussian-speciation trees principally in that strong imbalance and γ close to 0 are produced only under $\beta = 0.005$ and 0.01 and R_{shift} close to 0 (Fig. 3). This is consistent with the observation of high-I_c trees being generated under static skewed-speciation when $\beta = 0.005$ or 0.01. As with Gaussian-speciation (phase 2), the decline in mean I_c and γ with increasing R_{shift} coincides with a reduction in tree size which is, again, attributable to the inability of the diversification trait to keep up with the shifting diversification function. Here, however, the
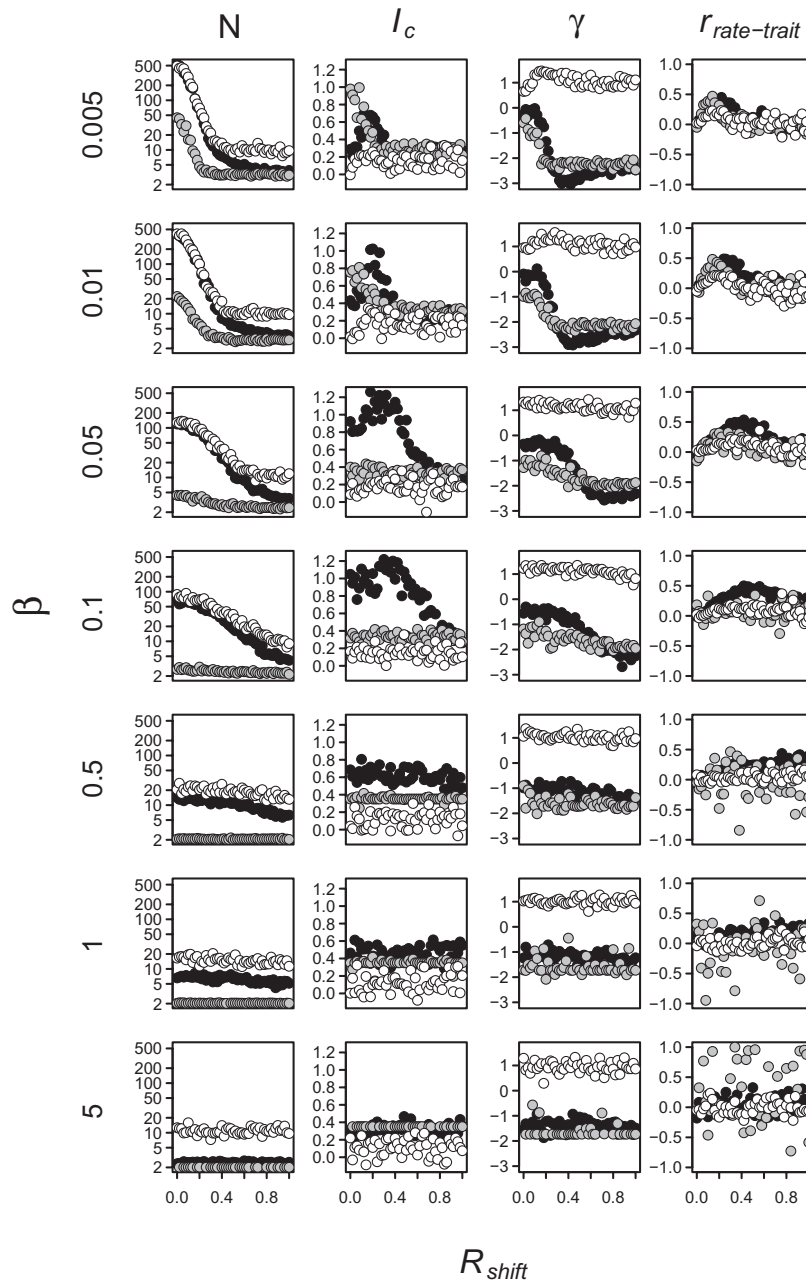
FIGURE 3. Variation in the mean size (species number, N; log-scale), mean Yule-normalized Colless' index (I_c) mean gamma statistic (γ), and mean diversification rate-trait correlation ($r_{rate-trait}$), plotted against the shift rate of the diversification function (R_{shift}), of trees generated under shifting Gaussian-speciation with $\mu = 0$ (black-filled circles), under shifting negatively skewed-speciation with $\mu = 0$ (gray-filled circles), and under shifting Gaussian-extinction with $\lambda = 0.6$ (open circles). Results are presented for $\beta = [0.005, 5]$ and only for simulations run under NDR_{max} ($\lambda_{max} - \mu$ or $\lambda - \mu_{min}$) = 0.6. Each point is a summary of trees generated by 100 replicate runs, excluding any runs going extinct or yielding a single species.

effect is more immediate owing to the narrowness of the skewed-speciation function. Interestingly, in contrast to mean I_c and γ, mean $r_{rate-trait}$ shows an initial increase with R_{shift}. Although we examined the effects of both negatively and positively skewed-speciation functions, we found no substantial differences and so present results only for the former.

Although trees generated under the "upside-down" Gaussian-extinction function show similar relationships

of mean I_c and $r_{rate-trait}$ to R_{shift} as do those generated under Gaussian-speciation, they differ in that the peak I_c and $r_{rate-trait}$ associated with R_{crit} are much more subdued (Fig. 3) and inconsistently significant (Supplementary Appendix 1 available on Dryad, Fig. 6). In terms of γ, however, Gaussian-extinction trees differ markedly from Gaussian-speciation trees, in having mean $\gamma > 0$. In a similar manner, Gaussian-speciation trees generated in the presence of random extinction ($\mu =$
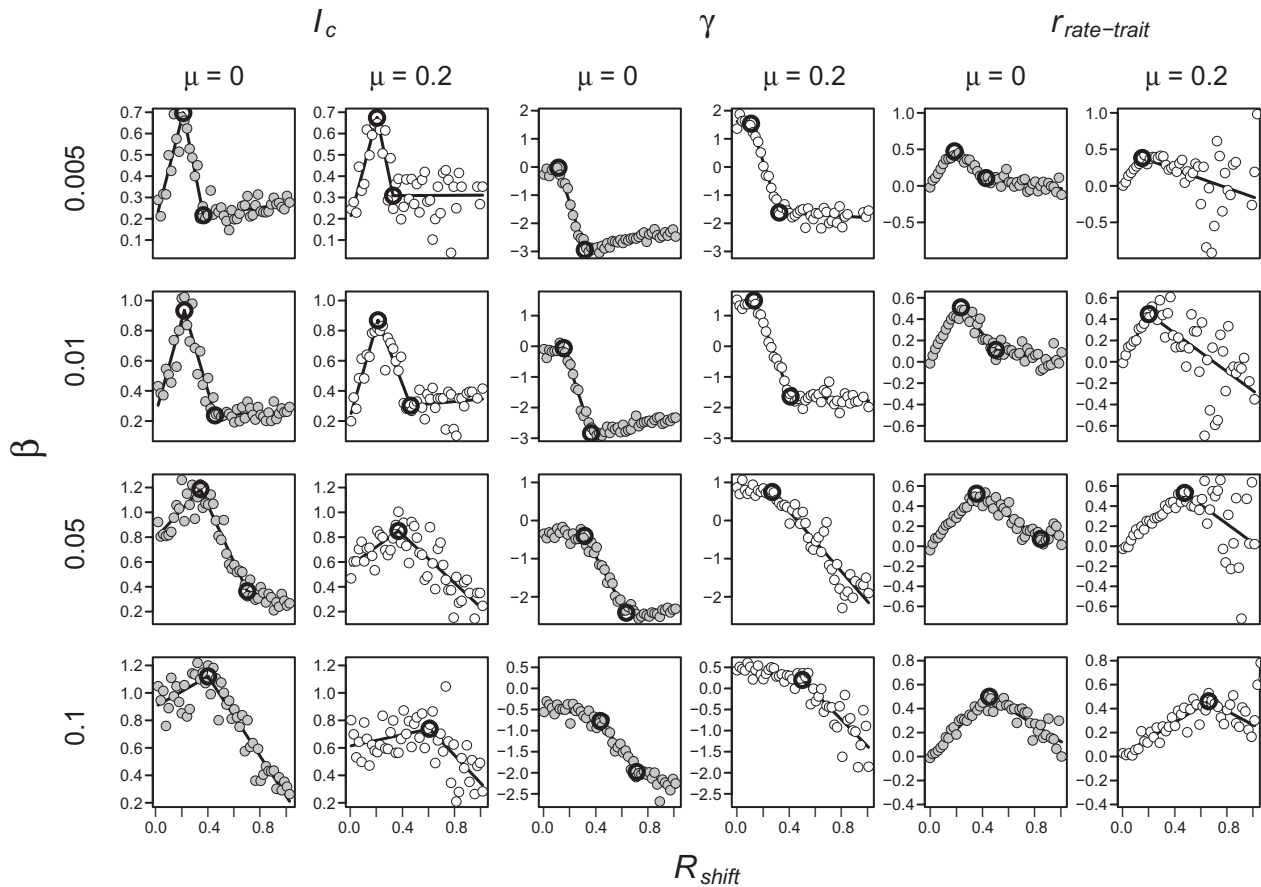
FIGURE 4.   Application of breakpoint regression to the relationships of mean Yule-normalized Colless' index (I_c), mean gamma statistic (γ), and mean diversification rate-trait correlation ($r_{rate-trait}$) to the shift rate of the diversification function (R_{shift}), for trees generated under Gaussian-speciation functions with $\mu = 0$ and $\mu = 0.2$. Results are presented for $\beta = [0.005, 0.1]$ and only for simulations run under $NDR_{max} = 0.6$. Each point is a summary of trees generated by 100 replicate runs, excluding any runs going extinct or yielding a single species. Bold circles indicate the positions of breakpoints identified as significant by the Davies (2002) test.

0.2) show subdued I_c signatures and higher γ relative to those generated under $\mu = 0$ (Supplementary Appendix 1 available on Dryad, Fig. 5).

Across the full range of R_{shift}, β, and NDR studied (simulation experiment 2), and considering only trees with ≥ 20 species ($N = 4241$), the sets of trees generated under the five diversification models (i.e., Gaussian-speciation with $\mu = 0$ and with $\mu = 0.2$; positively and negatively skewed-speciation; Gaussian-extinction) show separation in LDA ordination space but with considerable overlap, especially at low R_{shift} (Fig. 5). This separation, which is more apparent in large trees (≥ 100 species; Supplementary Appendix 1 available on Dryad, Fig. 7), is a consequence of significant differences (one-way ANOVA; $P < 0.001$ for all comparisons) in the I_c, γ, and $r_{rate-trait}$ signatures of these models (Fig. 6), which we summarize in Figure 7. Where $\gamma > 0$ is a typical outcome of diversification with extinction (i.e., Gaussian-extinction or Gaussian-speciation with extinction), $\gamma < 0$ is more typical of Gaussian- or skewed-speciation without extinction. Also, where high mean $r_{trait-rate}$ (e.g., > 0.25) is indicative of shifting species

selection under Gaussian- and skewed-speciation, both with and without background extinction, this is less true of Gaussian-extinction. Finally, where high mean I_c (e.g., > 0.5) is a common property of trees generated under Gaussian- or skewed-speciation, this is not a feature of trees generated under Gaussian-extinction.

Empirical Comparison

The 14 Cape plant phylogenies used to assess our model-based predictions have fynbos-association scores ranging from 0.38 (*Moraea*; species occur mostly in non-fynbos habitats) to 1.00 (*Tetraria*; species occur exclusively in fynbos) (Table 1). Within the same tree set, tree imbalance (I_c) ranges from -0.5 (*Tetraria*) to 8.32 (*Moraea*), while γ ranges from -4.15 (*Protea*) to 3.44 (*Gladiolus*). Consistent with our hypothesis, both I_c (linear regression: slope = -6.819 $P = 0.007$, adj. $r^2 = 0.428$) and γ (linear regression: slope = -5.867, $P = 0.037$, adj. $r^2 = 0.258$) are negatively related to fynbos-association score, with $\gamma > 0$ in lineages having low
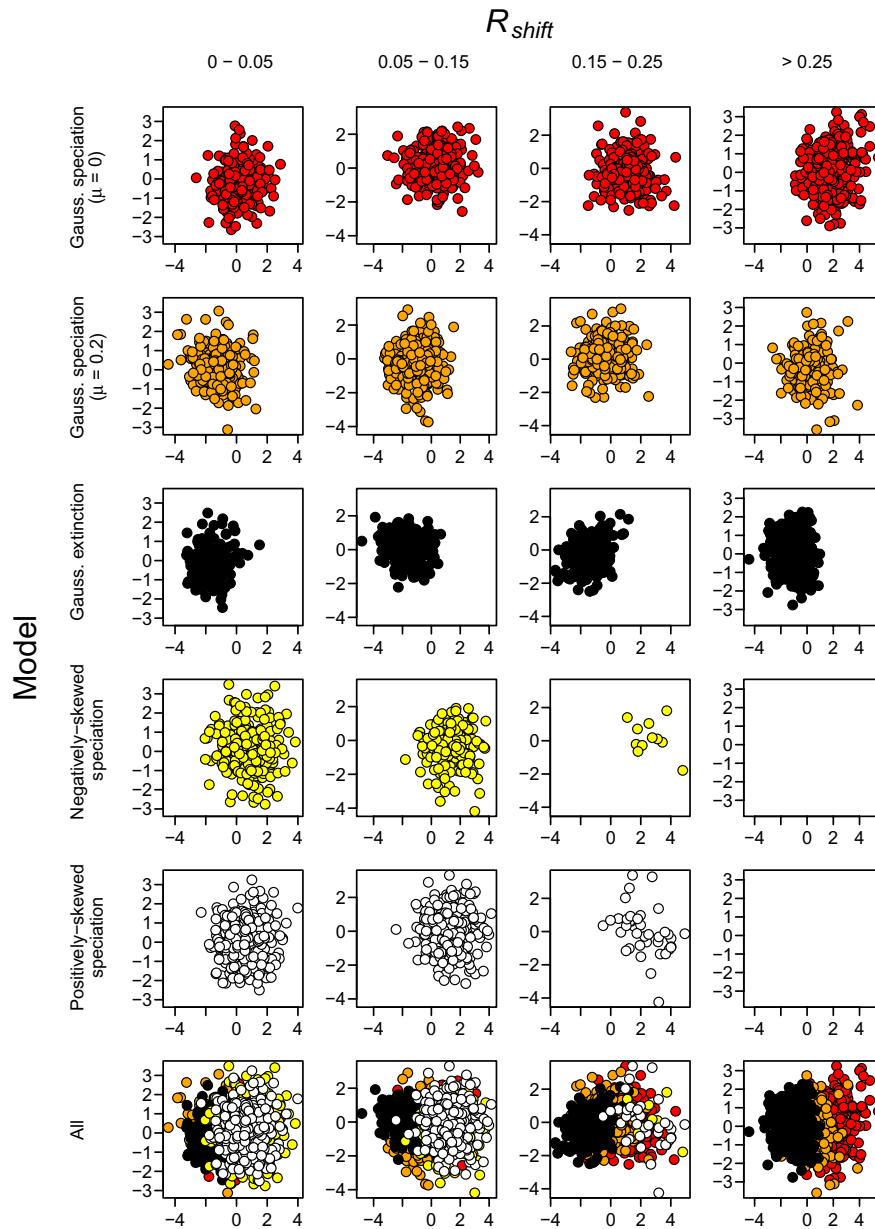
FIGURE 5. Ordinations of trees with ≥20 species generated under Gaussian-speciation (with $\mu = 0$ and $\mu = 0.2$), skewed-speciation (negatively and positively skewed), and Gaussian-extinction, based on linear discriminant analyses applied to I_c, γ, and $r_{rate-trait}$ scores. Separate analyses were done for $R_{shift} < 0.05$, $0.05 < R_{shift} < 0.15$, $0.15 < R_{shift} < 0.25$, and $R_{shift} > 0.25$, each column presenting the result of a different analysis. Within each column, the trees associated with each model are plotted separately (rows 1–5) and together (row 6). Within each plot the x- and y-axes describe the first and second linear discriminant functions, respectively.

fynbos-association scores and $\gamma < 0$ in lineages having strong fynbos associations (Fig. 8a,b). These patterns are robust to the omission of *Moraea* which occupies an outlying position in several plots (I_c: slope = -4.002, $P = 0.039$, adj. $r^2 = 0.273$; γ: slope = -8.289, $P = 0.007$ adj. $r^2 = 0.447$). In addition, consistent with the positive dependence of I_c on *NDR* observed in our simulations, the relationships of I_c to fynbos-association score are strengthened by the inclusion of tree size as a co-predictor (additive model), whether *Moraea* is

included in the comparison ($slope_{fynbos\ association\ score} = -6.783, P < 0.001; slope_{tree\ size} = 0.037$, $P = 0.001$, adj. $r^2 = 0.766$) or not ($slope_{fynbos\ association\ score} = -5.416, P = 0.006$; $slope_{tree\ size} = 0.026$, $P = 0.039$, adj. $r^2 = 0.489$).

Treating summer precipitation amount and precipitation seasonality as diversification traits we found that, where non-fynbos lineages tend to show negative $r_{rate-trait}$ with respect to summer precipitation amount and positive $r_{rate-trait}$ with respect to precipitation seasonality, this is not true for
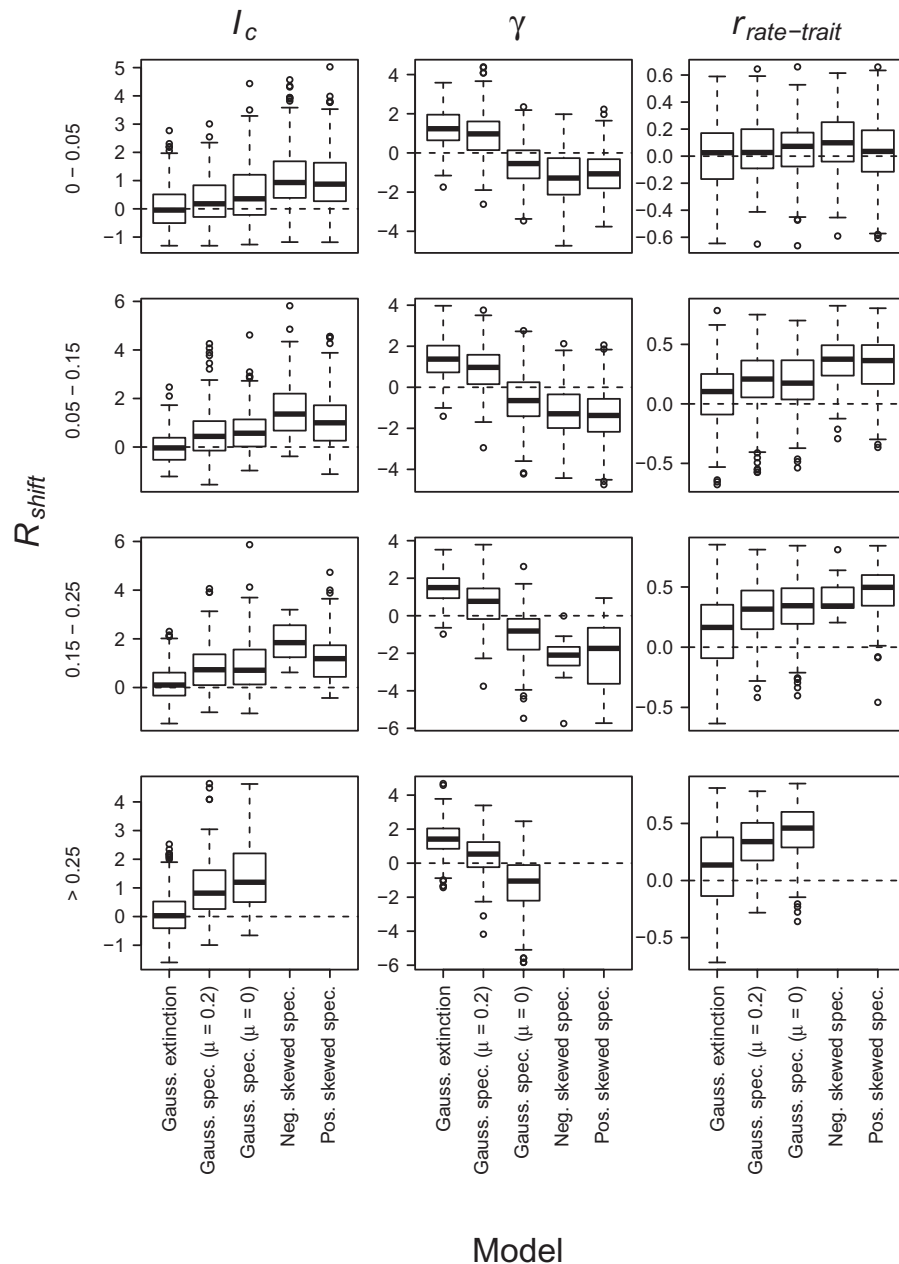
FIGURE 6.   Box and Whisker plots depicting the distributions of I_c, γ, and $r_{rate-trait}$ of trees with ≥ 20 species generated under Gaussian-speciation (with $\mu = 0$ and $\mu = 0.2$), skewed-speciation (negatively and positively skewed), and Gaussian-extinction. The data are presented separately for $R_{shift} < 0.05$, $0.05 < R_{shift} < 0.15$, $0.15 < R_{shift} < 0.25$, and $R_{shift} > 0.25$.

fynbos-associated lineages (Fig. 8c,d). These trends are significant, but only with the exclusion of *Moraea* (precipitation seasonality: slope = -0.846, $P = 0.019$, adj. $r^2 = 0.509$; driest quarter precipitation: slope = 0.986, $P = 0.016$, adj. $r^2 = 0.526$).

DISCUSSION

Species Selection Regime Affects Tree Shape

Empirical phylogenetic trees tend to be less balanced (e.g., Guyer and Slowinski 1993; Heard 1996; Blum and François 2006; Hagen et al. 2015; R et al. 2016) and have greater frequencies of deep branching events (Etienne and Rosindell 2012; Hagen et al. 2015; R et al. 2016) than trees generated under a constant birth–death process. Our simulations reveal that both these properties of empirical trees are generated by models that treat diversification as a trait-dependent process. Specifically, we show that trees generated under both Gaussian- and skewed-speciation achieve mean $I_c \gg 0$ and mean $\gamma \ll 0$ under some values of the trait diffusion parameter β. The latter, which represents the evolutionary rate of the

FIGURE 7.   Schematic summary indicating the mean Yule-normalized Colless' index (I_c), mean gamma statistic (γ), and mean diversification rate-trait correlation ($r_{rate-trait}$) of trees with ≥ 20 species, generated under static and shifting Gaussian-speciation, skewed-speciation, and Gaussian-extinction models, with $\mu = 0$ or $\mu > 0.2$ (speciation models only) and variable R_{shift}.

diversification trait, is of course critical in determining whether an evolving lineage is likely to occupy areas of trait space which describe both low and high rates of diversification, thereby fostering the diversification asymmetries that generate tree imbalance (cf. Heard 1996). Although the maximum imbalance levels reflected in Figs. 2–4 ($I_c \approx 1.2$) fall short of the highest levels observed empirically (e.g., Fig. 4 in Stadler et al. (2016)), this is partly because these figures reflect only the mean I_c of trees produced under each parameter combination. As reflected in Figure 6, the I_c scores of individual trees can be considerably higher. In addition, the strong linear dependence of mean I_c on NDR suggests that the mean I_c values generated by our simulations are limited by the range of diversification rates (NDR = [0.1, 0.6]) examined. For example, based on the relationship of mean I_c to NDR estimated under static Gaussian-speciation with $\mu = 0$ and $\beta = 0.1$ (i.e., mean $I_c = 1.520 * NDR - 0.031$), diversification rates of 1, 1.5, and 2 spp sp^{-1} myr^{-1} should yield trees with mean I_c = 1.49, 2.25, and 3.01, respectively. Diversification rates of this magnitude are considered "rapid" but have been reported from several plant groups (Klak et al. 2004; Valente et al. 2010).

In the absence of general expectations on the form of real species selection regimes (Freckleton et al. 2008; FitzJohn 2010), the ability of both Gaussian- (under $\beta = 0.05$, 0.1 and 0.5) and skewed-speciation (under $\beta = 0.005$ and 0.01) functions to generate appreciable I_c and γ signatures is reassuring in showing that the manifestation of these patterns is somewhat robust to variation in species selection regime. As implemented here, these functions represent distinct species selection scenarios. Where Gaussian-speciation best describes speciation within an adaptive zone whose ecological extent is normally distributed (cf. Pyron and Burbrink 2012), skewed-speciation better describes diversification under traits that influence genetic differentiation directly and for which the rate of differentiation is greatest under extreme trait values, such as dispersal rate, niche specificity and plant size (Jablonski 2008; Lengyel et al. 2009; Claramunt et al. 2012; Ebel et al. 2015; Boucher et al. 2017). Since the Gaussian distribution is a special case of the skewed-Gaussian distribution (i.e., with $\alpha = 0$), there is scope to model a diversity of intermediate species selection regimes, each maximizing tree imbalance under a slightly different value of β.
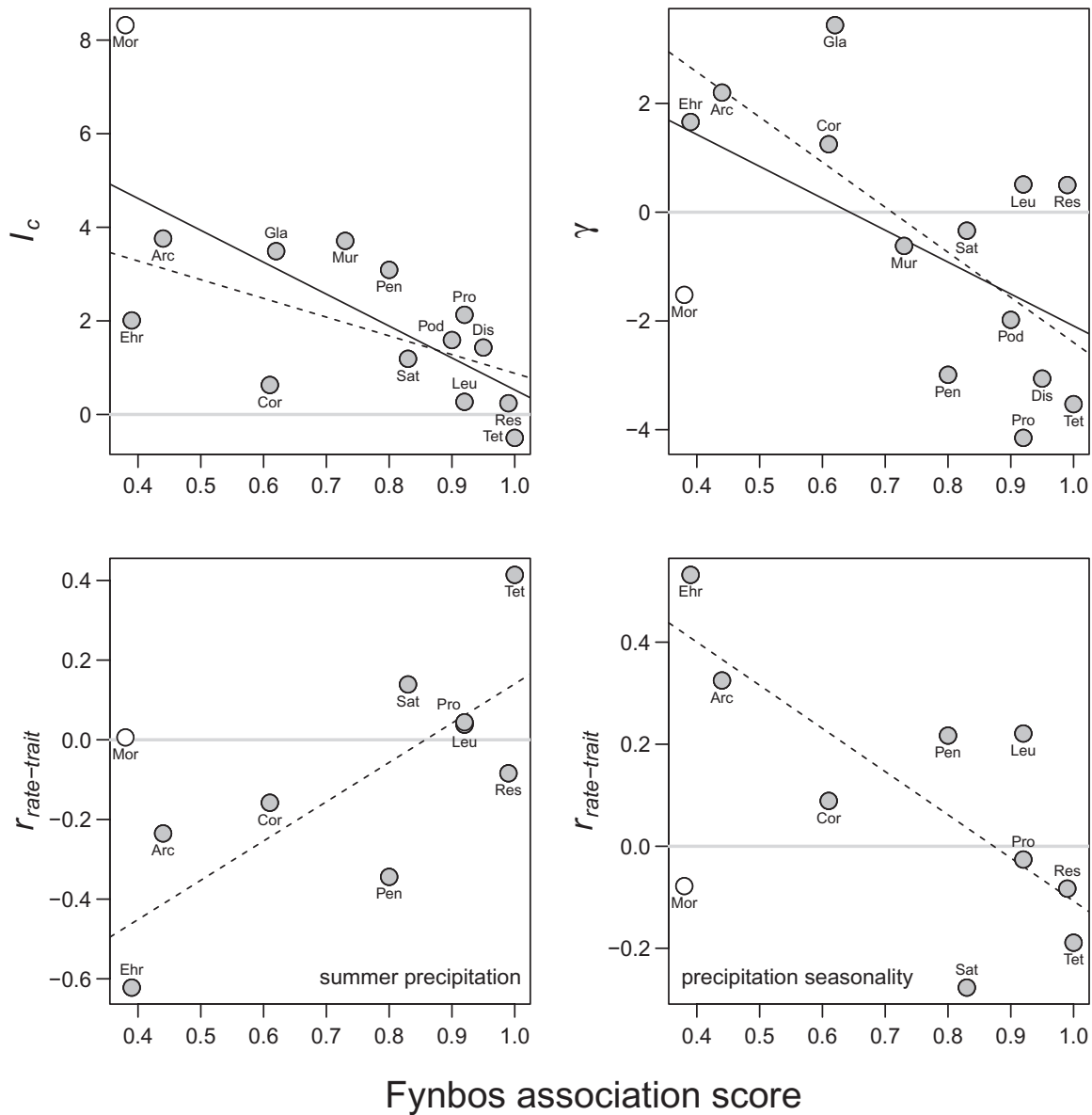
FIGURE 8.   Relationships of phylogenetic tree properties with vegetation association, across a suite of plant lineages from the Greater Cape Floristic Region of South Africa. Vegetation association is quantified as a fynbos-association score, ranging from 0 (lineage occurs exclusively in renosterveld or succulent karoo vegetation) to 1 (lineage occurs exclusively in fynbos vegetation). a and b) Relate the Yule-normalized Colless' index (I_c) and gamma statistic (γ) of each lineage's phylogenetic tree to its fynbos-association score, while c and d) relate the diversification rate-trait correlation ($r_{rate-trait}$) of each lineage to its fynbos-association score. The diversification traits in this case are mean summer precipitation amount (c) and precipitation seasonality (d). Solid lines depict relationships which are significant across all points, while dashed lines depict relationships that are significant only with the exclusion of *Moraea* (open circle). Lineage names are abbreviated as follows: Arc = Arctotidinae; Cor = *Corycium-Pterygodium*; Dsa = *Disa*; Ehr = *Ehrharta*; Gla = *Gladiolus*; Leu = *Leucadendron*; Mor = *Moraea*; Mur = *Muraltia*; Pen = *Pentameris*; Pod = Podalyrieae; Pro = *Protea*; Res = *Elegia-Thamnochortus*; Sat = *Satyrium*; Tet = *Tetraria*.

In contrast to Gaussian- and skewed-speciation functions, an "upside-down" Gaussian-extinction function, of the sort that underpins the greater longevity of morphologically average lineages (Liow 2007), does not appear to generate appreciable imbalance, particularly not when the function is static in time. The likely reason for this is that the high rates of extinction which come in to play when a lineage moves toward the margins of such a function can rapidly erase any imbalance previously generated by reduced extinction when the lineage was near the center of the diversification function. Indeed, our simulations reveal that extinction generally reduces the amount of signal in I_c relative to that obtained under $\mu = 0$, while simultaneously generating trees in which, consistent with theory (Pybus and Harvey 2000; Crisp and Cook 2009), branching events are consistently concentrated near the present (i.e., $\gamma > 0$). This has important

implications for understanding the biological processes underpinning imbalance in empirical phylogenetic trees. For example, where Farrell et al. (1991) suggested that the greater standing diversities of laticiferous plant clades relative to their sister clades might be a consequence of either increased speciation opportunity or reduced extinction risk associated with reduced herbivory, the failure of simulated trait-dependent extinction to generate substantial imbalance identifies differential speciation as a more likely explanation. In addition, the observation that extinction tends to erase the imbalance signature of species selection leads to the prediction of greater imbalance in recently radiated clades, in which extinction has not yet had the opportunity to act (i.e., "pull-of-the present"; Nee et al. 1994), than in older clades. Consistent with this expectation, Guyer and Slowinski (1991) found that the relationships of recently diverged, five-species clades were less balanced than those of five-species assemblages randomly sampled from the more-inclusive clades within which the five-species clades were embedded.

Shifting Species Selection Exacerbates Imbalance and Generates Trait-Rate Correlations

We predicted that, by consistently promoting diversification in lineages with extreme trait values, directionally shifting species selection should produce trees that are less balanced than those generated under a static species selection regime, and in which diversification rates are correlated with values of the underlying diversification trait(s). Our simulations confirm these predictions for trees generated under Gaussian-speciation and even under "upside-down" Gaussian-extinction, with the mean I_c and $r_{rate-trait}$ of trees generated under these functions increasing positively with R_{shift} up to a threshold value (R_{crit}). That the pattern for mean I_c is weak and inconsistent (Fig. 3; Supplementary Appendix 1 available on Dryad, Fig. 6) under Gaussian-extinction is unsurprising given the general tendency for extinction to erase imbalance signatures. R_{crit} itself represents the point beyond which the evolutionary rate of the diversification trait is insufficient to enable a lineage to keep up with the shifting species selection regime and, as such, is marked by a rapid decline in tree size and an associated loss of signal in I_c and $r_{rate-trait}$. This is the situation imposed on many species and supraspecific clades by rapid contemporary climate change (e.g., Parmesan 2006; Hof et al. 2011). That R_{crit} depends on the rate of evolution of the diversification trait (β) is unsurprising, but confirms the fundamental importance of a lineage's evolutionary lability, specifically in traits which influence speciation and extinction probability, in determining its capacity to persist in the face of environmental change (Chevin et al. 2010).

While our time-stratified shifting-peak model superficially resembles the linear diversification function implemented in QuaSSE (FitzJohn 2010) in modeling directional trait-dependent diversification, it differs in two important respects. Firstly, our model is temporally dynamic in that it allows the diversification function to shift over time. Secondly, the diversification function itself is nonlinear and converges to zero for extreme trait values. Besides conferring greater realism, given the dynamic nature of real species selection regimes (Uyeda et al. 2011; Hunt et al. 2014) and the apparently bounded nature of variation in most biological traits (e.g., Jensen and Zwieniecki 2013), these properties enable our model to capture two distinct sources of tree imbalance: that arising as a consequence of the form (i.e., Gaussian or skewed-Gaussian) of the diversification function and that produced by the temporally shifting nature of the species selection regime. Our data indicate that, while each of these effects is capable of generating imbalance in isolation, the highest levels of tree imbalance arise where both effects are in operation (e.g., Gaussian-speciation with $\beta = 0.1$ and $R_{shift} = R_{crit}$). Given that evolutionary dynamics over time are complex, involving both static and dynamic phases (Uyeda et al. 2011; Hunt et al. 2015), a consideration of both effects is important when attempting to account for imbalance levels in empirical phylogenetic trees.

In contrast to tree imbalance, our simulations suggest that diversification rate-trait correlations are uniquely an outcome of temporally shifting species selection. Our simulations are spatially inexplicit, however, and it seems likely that where space is substituted for time—that is, where lineage diversification takes place along a spatially structured environmental gradient rather than within a temporally changing environmental milieu—tree imbalance and rate-trait correlations should be equally apparent. Examples of this scenario include the radiation of *Androsace* from lowland ancestors in high-elevation alpine habitats in the Alps and the Himalayas (Roquet et al. 2013), and the radiation of *Viburnum* from tropical ancestors in a temperate setting (Spriggs et al. 2015). Importantly, though, whether the shift in species selection regime is temporal or spatial, the possibility exists of using rate-trait correlations, in conjunction with signatures of tree balance, to distinguish lineages which have diversified in the context of a changing selection regime from those which have not.

Tree Attributes Potentially Reveal Species Selection Regime

Although the tendency for contrasting species selection regimes to yield trees that differ in I_c, γ, and $r_{trait-rate}$ (Figs. 5–7) identifies tree shape as a potentially useful evolutionary diagnostic, some caution is warranted. Firstly, tree shape, as described by I_c and γ, is influenced by a host of processes other than those considered here, including the spatiotemporal dynamics of speciation process (Pigot et al. 2010; Etienne and Rosindell 2012; Hagen et al. 2015), mass extinction (Heard and Mooers 2002; Crisp and Cook 2009), clade-level diversity-dependent controls on diversification

(Rabosky and Lovette 2008), demographic stochasticity (Jabot and Chave 2009; Davies et al. 2011), and community-level biological interactions (Gascuel et al. 2015). Therefore, as with other macroevolutionary patterns (e.g., phylogenetic signal; Revell et al. 2008), there is a danger of ascribing a particular tree shape to the wrong generative process. However, we know of no process beyond trait-dependent diversification which can account for the rate-trait correlations that emerge under a temporally shifting diversification function (cf. Freckleton et al. 2008). Thus, given the evidence that lineage diversification is often trait-dependent and that environmental change, and the selective change that it implies, is a ubiquitous feature of most environments on Earth, species selection provides a particularly compelling explanation of tree shape as encapsulated by a combination of I_c, γ, and $r_{trait-rate}$.

A second factor compromising the utility of tree shape as a diagnostic of species selection regime is the overlap in I_c, γ, and $r_{trait-rate}$ of trees generated under contrasting species selection regimes. While these overlaps are often substantial (Figs. 5 and 6), they are probably exaggerated by our failure to partition trees generated under different values of NDR and β. In addition, given that these shape metrics are non-uniformly distributed for a particular tree set, the probability of generating a tree having a particular I_c, γ, and $r_{trait-rate}$ profile will likely vary amongst species selection scenarios, thus providing a means to resolve areas of overlap. In that context, we see a real need to develop a probabilistic framework within which the likelihoods of alternative diversification scenarios as explanations of a particular tree shape can be assessed. Although such a framework is beyond the scope of the present paper, we note that the time-stratified QuaSSE model implemented here provides a foundation, with a skewed-Gaussian distribution function offering the necessary flexibility to model not only alternative trait-dependent diversification scenarios (i.e., $\alpha = 0$ [Gaussian] or $|\alpha| >> 0$ [skewed]) but also trait-independent diversification ($\sigma_x^2 \to \infty$ or $\beta = 0$). Besides resolving overlaps in the shapes of trees generated under alternative diversification scenarios, the use of probabilistic models could allow for the evaluation of more complex diversification scenarios, including that in which trait-dependent speciation and extinction associate positively to cause high trait-dependent species turnover (e.g., Liow et al. 2008) and that in which multiple traits interact to produce a temporally dynamic, multimodal diversification landscape, analogous to the dynamic, multilocus adaptive landscapes of Wright (1932).

Cape Plant Phylogenies Reflect Contrasting Species Selection Regimes

Given limitations on the diagnostic utility of tree shape as outlined in the preceding section, it is remarkable how well the phylogenies of Cape plant lineages, which have variously diversified in stable fynbos environments versus more-changeable non-fynbos environments, match our theoretical expectations. Consistent with our expectations, the phylogenetic trees of fynbos-associated lineages generally have I_c and γ close to 0, with little evidence of a correlation between diversification rate and either driest-quarter (i.e., summer) precipitation or precipitation seasonality ($r_{rate-trait} \approx 0$). Based on the range of model parameters explored in our simulations, these characteristics are most consistent with diversification under a relatively static species selection regime with negligible extinction (Fig. 7). This aligns closely with suggestions that the exceptional richness and low-dispersibility of the fynbos flora, particularly the montane flora (Cowling and Lombard 2002), is a consequence of low extinction risk associated with minimal climatic perturbation through the Pleistocene and earlier (Dynesius and Jansson 2000; Latimer et al. 2005; Kreft and Jetz 2007; Linder 2008). That the exceptionally low I_c (≈ 0) of some lineages (e.g., *Elegia-Thamnochortus*, *Tetraria*) is more consistent with a constant rather than a trait-dependent Gaussian- or skewed-diversification model is initially surprising. However, given that the latter models converge on the constant model as β tends toward 0, this could reflect the exceptionally limited evolutionary flexibility (i.e., low β) of fynbos plant traits which may be a consequence of extreme specialization to low-nutrient settings (Power et al. 2017; Verboom et al. 2017).

In contrast to fynbos lineages, the phylogenetic trees of succulent karoo/renosterveld-associated lineages have I_c and $\gamma > 0$, with diversification being related to both precipitation seasonality ($r_{rate-trait} > 0$) and summer precipitation amount ($r_{rate-trait} < 0$). Taken together, these features are suggestive of diversification in the context of a shifting species selection regime, underpinned by a trend toward increasingly arid summers and involving some extinction (Fig. 7). This accords closely with suggestions that the low-elevation flora of the western GCFR is a product of rapid radiation stimulated by climatic deterioration since the Late Miocene-Pliocene (Levyns 1964; Linder 2008; Verboom et al. 2009, 2014), a scenario which, consistent with Vrba (1985) turnover pulse hypothesis, would have involved significant extinction and species turnover (e.g., Linder et al. 1992). Although a direct assessment of the relationship between diversification rates and environmental change over time (cf. Condamine et al. 2013) would provide valuable corroboration, the lack of a continuous, regional precipitation record for the past 10 myr places this out of reach.

Although the relationships of $r_{rate-trait}$ to fynbos-association score are generally low on account of the presence of an outlier lineage (*Moraea*), this is scarcely surprising given that lineage diversification is influenced by a diversity of interacting environmental variables and traits (De Queiroz 2002; Donoghue and Sanderson 2015). Within the GCFR, for example, diversification is

influenced by a range of environmental factors other than summer precipitation amount and precipitation seasonality (e.g., soils, fire, pollinators; Ellis et al. 2014), the relative importance of these factors as diversification stimuli varying between lineages on account of their different functional attributes.

Species Selection Regime: A General Explanation of Tree Shape?

Our data, both simulated and empirical, suggest an important role for historical species selection in shaping organismal phylogenies, thus supporting the notion that "questions about variation in diversification rates among clades are fundamentally questions about species selection" (Rabosky and McCune 2009). The broader significance of this conclusion lies in the observation that most biological diversity has evolved in the context of a spatiotemporally variable global environment, in which both species distributions and lineage diversification are commonly trait-modulated. The Neogene, for example, has witnessed dramatic global-scale climate change (Zachos et al. 2001) which, in conjunction with events taking place at local or regional scales (e.g., regional tectonism; Harrison et al. 1992; Hoorn et al. 2010), has prompted major vegetation rearrangement and floristic turnover at a variety of scales (e.g., Cerling et al. 1997; Simon et al. 2009; Luebert and Weigend 2014). On the evidence of analyses presented here, these changes would undoubtedly have left their signature on the shapes of phylogenetic trees and in the distributions of traits influencing diversification. This, then, opens the possibility of using tree shape to gain insights into paleoenvironmental history. Where phylogenetic approaches have been developed which provide insights into the shape and dynamics of the adaptive landscapes that underpin selection at the microevolutionary level (Ingram and Mahler 2013; Uyeda and Harmon 2014), our work draws attention to the promise of using phylogenies to reveal the form and dynamics of selective regimes operating above the species level (i.e., species selection).

SUPPLEMENTARY MATERIAL

Data available from the Dryad Digital Repository: http://dx.doi.org/10.5061/dryad.1sf007b.

REFERENCES

Ackerly D. 2009. Conservatism and diversification of plant functional traits: evolutionary rates versus phylogenetic signal. Proc. Natl. Acad. Sci. USA. 106(Suppl 2):19699–19706.

Arnold S.J., Pfrender M.E., Jones A.G. 2001. The adaptive landscape as a conceptual bridge between micro- and macroevolution. Genetica. 112–113:9–32.

Bergh N.G., Verboom G.A., Rouget M., Cowling R.M. 2014. Vegetation types of the Greater Cape Floristic Region. In: Allsopp N., Colville J.F., Verboom G.A., editors. Fynbos: ecology, evolution and conservation of a megadiverse region. Oxford: Oxford University Press. p. 1–25.

Blum M.G., François O. 2006. Which random processes describe the tree of life? A large-scale study of phylogenetic tree imbalance. Syst. Biol. 55:685–691.

Boucher F.C., Verboom G.A., Musker S.D., Ellis A.G. 2017. Plant size: a key determinant of diversification? New Phytol. 216: 24–31.

Brodribb T.J., Field T.S. 2010. Leaf hydraulic evolution led a surge in leaf photosynthetic capacity during early angiosperm diversification. Ecol. Lett. 13:175–183.

Brodribb T.J., McAdam S.A.M., Jordan G.J., Field T.S. 2009. Evolution of stomatal responsiveness to CO_2 and optimization of water-use efficiency among land plants. New Phytol. 183:839–847.

Bytebier B., Antonelli A., Bellstedt D.U., Linder H.P. 2010. Estimating the age of the Cape flora of South Africa from an orchid phylogeny. Proc. R. Soc. B. 278:188–195.

Cerling T.E., Harris J.M., MacFadden B.J., Leakey M.G., Quade J., Eisenmatt V., Ehleringer J.R. 1997. Global vegetation change through the Miocene/Pliocene boundary. Nature. 389:153–158.

Chan K.M.A., Moore B.R. 2002. Whole-tree methods for detecting differential diversification rates. Syst. Biol. 51:855–865.

Chevin L.-M. 2016. Species selection and random drift in macroevolution. Evolution. 70:513–525.

Chevin L.-M., Lande R., Mace G.M. 2010. Adaptation, plasticity, and extinction in a changing environment: towards a predictive theory. PLoS Biol. 8:e1000357.

Claramunt S., Derryberry E.P., Remsen J.V. Jr., Brumfield R.T. 2012. High dispersal ability inhibits speciation in a continental radiation of passerine birds. Proc. R. Soc. B. 279:1567–1574.

Colless D.H. 1982. Phylogenetics: the theory and practice of phylogenetic systematics. Syst. Zool. 31:100–104.

Condamine F.L., Rolland J., Morlon H. 2013. Macroevolutionary perspectives to environmental change. Ecol. Lett. 16:72–85.

Coyne J.A., Orr H.A. 2004. Speciation. Sunderland (MA): Sinauer.

Cowling R.M., Lombard A.T. 2002. Heterogeneity, speciation/ extinction history and climate: explaining regional plant diversity patterns in the Cape Floristic Region. Divers. Distrib. 8:163–179.

Cowling R.M., Proches Ş., Partridge T.C. 2009. Explaining the uniqueness of the Cape flora: incorporating geomorphic evolution as a factor for explaining its diversification. Mol. Phylogenet. Evol. 51:64–74.

Crawley M.J. 2007. The R book. Chichester: John Wiley and Sons.

Crisp M.D., Cook L.G. 2009. Explosive radiation or crypic mass extinction? Interpreting signatures in molecular phylogenies. Evolution. 63:2257–2265.

Darwin F., Seward A.C., editors. 1903. More letters of Charles Darwin, Vol. 2. London: John Murray.

Davies R.B. 2002. Hypothesis testing when a nuisance parameter is present only under the alternative: linear model case. Biometrika. 89:484–489.

Davies T.J., Allen A.P., Borda-de-Água L., Regetz J., Melián C.J. 2011. Neutral biodiversity theory can explain the imbalance of phylogenetic trees but not the tempo of their diversification. Evolution. 65:1841–1850.

Davies T.J., Barraclough T.G., Chase M.W., Soltis P.S., Soltis D.E., Savolainen V. 2004. Darwin's abominable mystery: Insights from a supertree of the angiosperms. Proc. Natl. Acad. Sci. USA. 101:1904–1909.

De Queiroz A. 2002. Contingent predictability in evolution: key traits and diversification. Syst. Biol. 51:917–929.

Donoghue M.J., Sanderson M.J. 2015. Confluence, synnovation, and depauperons in plant diversification. New Phytol. 207: 260–274.

Dupont L.M., Linder H.P., Rommerskirchen F., Schefuß E. 2011. Climate-driven rampant speciation of the Cape flora. J. Biogeogr. 38:1059–1068.

Dynesius M., Jansson R. 2000. Evolutionary consequences of changes in species' geographical distributions driven by Milankovitch climate oscillations. Proc. Natl. Acad. Sci. USA. 97:9115–9120.

Ebel E.R., Dacosta J.M., Sorenson M.D., Hill R.I., Briscoe A.D., Willmott K.R., Mullen S.P. 2015. Rapid diversification associated with ecological specialization in Neotropical *Adelpha* butterflies. Mol. Ecol. 24:2392–2405.

Eldredge N., Cracraft J. 1980. Phylogenetic patterns and evolutionary process. New York (NY): Columbia University Press.

Ellis A.G., Verboom G.A., van der Niet T., Johnson S.D., Linder H.P. 2014. Speciation and extinction in the Greater Cape Floristic Region. In: Allsopp N., Colville J.F., Verboom G.A., editors. Fynbos: ecology, evolution and conservation of a megadiverse region. Oxford: Oxford University Press. p. 119–141.

Etienne R.S., Rosindell J. 2012. Prolonging the past counteracts the pull of the present: protracted speciation can explain observed slowdowns in diversification. Syst. Biol. 61:204–213.

Farrell B.D., Dussourd D.E., Mitter C. 1991. Escalation of plant defense: do latex and resin canals spur plant diversification? Am. Nat. 138:881–900.

Fish L., Mashau A.C., Moeaha M.J., Nembudani M.T. 2015. Identification guide to Southern African grasses. Pretoria: South African National Biodiversity Institute.

FitzJohn R.G. 2010. Quantitative traits and diversification. Syst. Biol. 59:619–633.

FitzJohn R.G. 2012a. What drives biological diversification? Detecting traits under species selection [PhD dissertation]. University of British Columbia.

FitzJohn R.G. 2012b. Diversitree: comparative phylogenetic analyses of diversification in R. Methods Ecol. Evol. 3:1084–1092.

FitzJohn R.G., Maddison W.P., Otto S.P. 2009. Estimating trait-dependent speciation and extinction rates from incompletely resolved phylogenies. Syst. Biol. 58:595–611.

Forest F., Nänni I., Chase M.W., Crane P.R., Hawkins J.A. 2007. Diversification of a large genus in a continental biodiversity hotspot: temporal and spatial origin of *Muraltia* (Polygalaceae) in the Cape of South Africa. Mol. Phylogenet. Evol. 43:60–74.

Franks P.J., Beerling D.J. 2009. Maximum leaf conductance driven by CO_2 effects on stomatal size and density over geologic time. Proc. Natl. Acad. Sci. USA. 106:10343–10347.

Freckleton R.P., Phillimore A.B., Pagel M. 2008. Relating traits to diversification: a simple test. Am. Nat. 172:102–115.

Freyman W.A., Höhna S. 2019. Stochastic character mapping of state-dependent diversification reveals the tempo of evolutionary decline in self-compatible Onagraceae lineages. Syst. Biol. 68:505–519.

Gascuel F., Ferrière R., Aguilée R., Lambert A. 2015. How ecology and landscape dynamics shape phylogenetic trees. Syst. Biol. 64: 590–607.

Goldberg E.E., Kohn J.R., Lande R., Robertson K.A., Smith S.A., Igić B. 2010. Species selection maintains self-incompatibility. Science. 330:493–495.

Goldblatt P. 1979. Biology and systematics of *Galaxia* (Iridaceae). J. S. Afr. Bot. 45:385–423.

Goldblatt P. 1981. Systematics and biology of *Homeria* (Iridaceae). Ann. Missouri Bot. Gard. 68:413–503.

Goldblatt P. 1986. The moraeas of southern Africa. (South Africa), Cape Town: National Botanic Gardens.

Goldblatt P., Manning J.C. 1998. *Gladiolus* in southern Africa. Cape Town: Fernwood Press.

Guyer C., Slowinski J.B. 1991. Comparisons of observed phylogenetic topologies with null expectations among three monophyletic lineages. Evolution. 45:340–350.

Guyer C., Slowinski J.B. 1993. Adaptive radiation and the topology of large phylogenies. Evolution. 47:253–263.

Hagen O., Hartmann K., Steel M., Stadler T. 2015. Age-dependent speciation can explain the shape of empirical phylogenies. Syst. Biol. 64:432–440.

Harmon L.J., Weir J.T., Brock C.D., Glor R.E., Challenger W. 2008. GEIGER: investigating evolutionary radiations. Bioinformatics. 24:129–131.

Harrison T.M., Copeland P., Kidd W.S.F., Yin A. 1992. Raising Tibet. Science. 255:1663–1670.

Heard S.B. 1996. Phylogenetic tree balance with variable and evolving speciation rates. Evolution. 50:2141–2148.

Heard S.B., Hauser D.L. 1995. Key evolutionary innovations and their ecological mechanisms. Hist. Biol. 10:151–173.

Heard S.B., Mooers A.Ø. 2002. Signatures of random and selective mass extinctions in phylogenetic tree balance. Syst. Biol. 51:889–897.

Hijmans R.J. 2016. Raster: geographic data analysis and modeling. R package version 2.5-8. https://CRAN.R-project.org/package=raster.

Hof C., Levinsky I., Araújo M.B., Rahbek C. 2011. Rethinking species' ability to cope with rapid climate change. Global Change Biol. 17:2987–2990.

Hoffmann V., Verboom G.A., Cotterill F.P.D. 2015. Dated plant phylogenies resolve Neogene climate and landscape evolution in the Cape Floristic Region. PLoS One. 10:e0137847.

Hoorn C., Wesselingh F.P., ter Steege H., Bermudez M.A., Mora A., Sevink J., Sanmartín I., Sanchez-Meseguer A., Anderson C.L., Figueiredo J.P., Jaramillo C., Riff D., Negri F.R., Hooghiemstra H., Lundberg J., Stadler T., Särkinen T., Antonelli A. 2010. Amazonia through time: Andean uplift, climate change, landscape evolution, and biodiversity. Science. 330:927–931.

Hunt G., Hopkins M.J., Lidgard S. 2015. Simple versus complex models of trait evolution and stasis as a response to environmental change. Proc. Natl. Acad. Sci. USA. 112:4885–4890.

Ingram T., Mahler D.L. 2013. SURFACE: detecting convergent evolution from comparative data by fitting Orstein-Uhlenbeck models with stepwise Akaike Information Criterion. Methods Ecol. Evol. 4:416–425.

Jablonski D. 2008. Species selection: theory and data. Annu. Rev. Ecol. Evol. Syst. 39:501–524.

Jabot F., Chave J. 2009. Inferring the parameters of the neutral theory of biodiversity using phylogenetic information and implications for tropical forests. Ecol. Lett. 12:239–248.

Jensen K.H., Zwieniecki M.A. 2013. Physical limits to leaf size in tall trees. Phys. Rev. Lett. 110:018104.

Johnson M.T., FitzJohn R.G., Smith S.D., Rausher M.D., Otto S.P. 2011. Loss of sexual recombination and segregation is associated with increased diversification in evening primroses. Evolution. 65:3230–3240.

Kembel S.W., Cowan P.D., Helmus M.R., Cornwell W.K., Morlon H., Ackerly D.D., Blomberg S.P., Webb C.O. 2010. Picante: R tools for integrating phylogenies and ecology. Bioinformatics. 26:1463–1464.

Klak C., Reeves G., Hedderson T. 2004. Unmatched tempo of evolution in Southern African semi-desert ice plants. Nature. 427:63–65.

Kreft H., Jetz W. 2007. Global patterns and determinants of vascular plant diversity. Proc. Natl. Acad. Sci. USA. 104:5925–5930.

Landis M.J. 2017. Biogeographic dating of speciation times using paleogeographically informed processes. Syst. Biol. 66:128–144.

Latimer A.M., Silander J.A. Jr., Cowling R.M. 2005. Neutral ecological theory reveals isolation and rapid speciation in a biodiversity hotspot. Science. 309:1722–1725.

Lengyel S., Gove A.D., Latimer A.M., Majer J.D., Dunn R.R. 2009. Anst sow the seeds of global diversification in flowering plants. PLoS One. 4:e5480.

Levyns M.R. 1954. The genus *Muraltia*. J. S. Afr. Bot. 2(Suppl): 1–247.

Levyns M.R. 1964. Presidential address: migrations and origin of the Cape flora. Trans. R. Soc. South Africa. 37:85–107.

Liltved W.R., Johnson S.D. 2012. The Cape orchids. Cape Town: Sandstone Editions.

Linder H.P. 1991. A revision of *Pentaschistis* (Arundineae: Poaceae). Contributions from the Bolus Herbarium, Vol. 12. Cape Town: University of Cape Town. p. 1–124.

Linder H.P. 2003. The radiation of the Cape flora, southern Africa. Biol. Rev. 78:597–638.

Linder H.P. 2006. The African Restionaceae, version 4. Controbutions from the Bolus Herbarium 20 (Interactive key on CD ROM). Cape Town: University of Cape Town.

Linder H.P. 2008. Plant species radiations: where, when, why? Philos. Trans. R. Soc. B. 363:3097–3105.

Linder H.P., Kurzweil H. 1999. Orchids of southern Africa. Rotterdam: Balkema.

Linder H.P., Meadows M.E., Cowling R.M. 1992. History of the Cape flora. In: Cowling R.M., editors. Ecology of fynbos: nutrients, fire and diversity. Cape Town: Oxford University Press. p. 113–134.

Liow L.H. 2007. Lineages with long durations are morphologically average: an analysis using multiple datasets. Evolution. 61:885–901.

Liow L.H., Fortelius M., Bingham E., Lintulaakso K., Flynn L., Stenseth N.C. 2008. Higher origination and extinction rates in larger mammals. Proc. Natl. Acad. Sci. USA. 105:6097–6102.

Luebert F., Weigend M. 2014. Phylogenetic insights into Andean plant diversification. Front. Ecol. Evol. 2:27.

Maddison W.P., Midford P.E., Otto S.P. 2007. Estimating a binary character's effect on speciation and extinction. Syst. Biol. 56:701–710.

Magallón S., Sanderson M.J. 2001. Absolute diversification rates in angiosperm clades. Evolution. 55:1762–8170.

Manning J.C., Goldblatt P. 2012. Plants of the Greater Cape Floristic Region 1: the Core Cape Region. Pretoria: South African National Biodiversity Institute.

Muggeo V.M.R. 2003. Estimating regression models with unknown break-points. Stat. Med. 22:3055–3071.

Muggeo V.M.R. 2008. Segmented: an R package to fit regression models with broken-line relationships. R News 8/1:20-2.

Nee S., May R.M., Harvey P.H. 1994. The reconstructed evolutionary process. Philos. Trans. R. Soc. B. 344:305–311.

Oliver M.J., Petrov D., Ackerly D., Falkowski P., Schofield O.M. 2007. The mode and tempo of genome size evolution in eukaryotes. Genome Res. 17:594–601.

Paradis E., Claude J., Strimmer K. 2004. APE: analyses of phylogenetics and evolution in R language. Bioinformatics. 20:289–290.

Parkhurst D.F., Loucks O.L. 1972. Optimal leaf size in relation to environment. J. Ecol. 60:505–537.

Parmesan C. 2006. Ecological and evolutionary response to recent climate change. Annu. Rev. Ecol. Evol. Syst. 37:637–669.

Pigot A.L., Phillimore A.B., Owens I.P.F., Orme C.D.L. 2010. The shape and temporal dynamics of phylogenetic trees arising from geographic speciation. Syst. Biol. 59:660–673.

Power S.C., Verboom G.A., Bond W.J., Cramer M.D. 2017. Environmental correlates of biome-level floristic turnover in South Africa. J. Biogeogr. 44:1745–1757.

Pybus O.G., Harvey P.H. 2000. Testing macro-evolutionary models using incomplete molecular phylogenies. Proc. Biol. Sci. 267:2267–2272.

Pyron R.A., Burbrink F.T. 2012. Trait-dependent diversification and the impact of palaeontological data on evolutionary hypothesis testing in New World ratsnakes (tribe Lampropeltini). J. Evol. Biol. 25:497–508.

R Core Team. 2016. R: A language and environment for statistical computing. R Foundation for Statistical Computing, Vienna, Austria. https://www.R-project.org/.

Rabosky D.L., Lovette I.J. 2008. Density-dependent diversification in North American wood warblers. Proc. R. Soc. B. 275:2363–2371.

Rabosky D.L., McCune A.R. 2009. Reinventing species selection with molecular phylogenies. Trends Ecol. Evol. 25:68–74.

Rebelo A. 2001. SASOL proteas: a field guide to the proteas of southern Africa. 2nd ed. Cape Town: Fernwood Press.

Ree R.H., Smith S.A. 2008. Maximum likelihood inference of geographic range evolution by dispersal, local extinction, and cladogenesis. Syst. Biol. 57:4–14.

Revell L.J. 2012. Phytools: an R package for phylogenetic comparative biology (and other things). Methods Ecol. Evol. 3:217–223.

Revell L.J., Harmon L.J., Collar D.C. 2008. Phylogenetic signal, evolutionary process, and rate. Syst. Biol. 57:591–601.

Ridley M. 2003. Evolution. 3rd ed. Oxford: Blackwell.

Roquet C., Boucher F.C., Thuiller W., Lavergne S. 2013. Replicated radiations of the alpine genus Androsace (Primulaceae) driven by range expansion and covergent key innovations. J. Biogeogr. 40:1874–1886.

Rourke J.P. 1980. The proteas of southern Africa. Cape Town: Purnell.

Sanderson M.J., Donoghue M.J. 1994. Shifts in diversification rate with the origin of angiosperms. Science. 264:1590–1593.

Scharf T.E., Codilean A.T., de Wit M., Jansen J.D., Kubik P.W. 2013. Strong rocks sustain ancient postorogenic topography in southern Africa. Geology. 41:331–334.

Schnitzler J., Barraclough T.G., Boatwright J.S., Goldblatt P., Manning J.C., Powell M.P., Rebelo T., Savolainen V. 2011. Causes of plant diversification in the Cape biodiversity hotspot of South Africa. Syst. Biol. 60:343–357.

Schutte A.L. 1997a. A revision of the genus Xiphotheca (Fabaceae). Ann. Missouri Bot. Gard. 84:90–102.

Schutte A.L. 1997b. Systematics of the genus Liparia. Nordic J. Bot. 17:11–37.

Schutte A.L., van Wyk B.E. 2011. A taxonomic revision of Podalyria (Fabacee). Syst. Bot. 36:631–660.

Simpson G.G. 1944. Tempo and mode in evolution. New York (NY): Columbia University Press.

Simpson G.G. 1953. The major features of evolution. New York (NY): Columbia University Press.

Slingsby J.A., Britton M.N., Verboom G.A. 2014. Ecology limits the diversity of the Cape flora: phylogenetics and diversification of the genus Tetraria. Mol. Phylogenet. Evol. 72:61–70.

Slowinski J.B., Guyer C. 1993. Testing whether certain traits have caused amplified diversification: an improved method based on a model of random speciation and extinction. Am. Nat. 142: 1019–1024.

Snijman D.A., editors. 2013. Plants of the Greater Cape Floristic Region 2: the extra Cape Flora. Pretoria: South African National Biodiversity Institute.

Spriggs E.L., Clement W.L., Sweeney P.W., Madriñán S., Edwards E.J., Donoghue M.J. 2015. Temperate radiations and dying embers of a tropical past: the diversification of Viburnum. New Phytol. 207:340–354.

Stadler T., Degnan J.H., Rosenberg N.A. 2016. Does gene tree discordance explain the mismatch between macroevolutionary models and empirical patterns of tree shape and branching times? Syst. Biol. 65:628–639.

Stanley S.M. 1975. A theory of evolution above the species level. Proc. Natl. Acad. Sci. USA. 72:646–650.

Uyeda J.C., Hansen T.F., Arnold S.J., Pienaar J. 2011. The million-year wait for macroevoluntary bursts. Proc. Natl. Acad. Sci. USA. 108:15908–15913.

Uyeda J.C., Harmon L.J. 2014. A novel Bayesian method for inferring and interpreting the dynamics of adaptive landscapes from phylogenetic comparative data. Syst. Biol. 63:902–918.

Valente L.M., Savolainen V., Vargas P. 2010. Unparalleled rates of species diversification in Europe. Proc. R. Soc. B. 277:1489–1496.

Valente L.M., Savolainen V., Manning J.C., Goldblatt P., Vargas P. 2011. Explaining disparities in species richness between Mediterranean floristic regions: a case study in Gladiolus (Iridaceae). Global Ecol. Biogeogr. 20:881–892.

Verboom G.A., Archibald J.K., Bakker F.T., Bellstedt D.U., Conrad F., Dreyer L.L., Forest F., Galley C., Goldblatt P., Henning J.F., Mummenhoff K., Peter Linder H., Muthama Muasya A., Oberlander K.C., Savolainen V., Snijman D.A., van derNiet T., Nowell T.L. 2009. Origin and diversification of the Greater Cape flora: ancient species repository, hot-bed of recent radiation, or both? Mol. Phylogenet. Evol. 51:44–53.

Verboom G.A., Bergh N.G., Haiden S.A., Hoffmann V., Britton M.N. 2015. Topography as a driver of diversification in the Cape Floristic Region of South Africa. New Phytol. 207:368–376.

Verboom G.A., Linder H.P., Forest F., Hoffmann V., Bergh N.G., Cowling R.M. 2014. Cenozoic assembly of the Greater Cape Flora. In: Allsopp N., Colville J.F., Verboom G.A., editors. Fynbos: ecology, evolution and conservation of a megadiverse region. Oxford: Oxford University Press. p. 93–118.

Verboom G.A., Stock W.D., Cramer M.D. 2017. Specialization to extremely low-nutrient soils limits the nutritional adaptability of plant lineages. Am. Nat. 189:684–699.

Vrba E.S. 1984. What is species selection? Syst. Zool. 33:318–328.

Vrba E.S. 1985. Environment and evolution: alternative causes of the temporal distribution of evolutionary events. S. Afr. J. Sci. 81:229–236.

Westoby M., Jurado E., Leishman M. 1992. Comparative evolutionary ecology of seed size. Trends Ecol. Evol. 7:369–372.

Williams I.J.M. 1972. A revision of the genus *Leucadendron* (Proteaceae). Contributions from the Bolus Herbarium, Vol 3. Cape Town: University of Cape Town. p. 1–425.

Wright S. 1931. Evolution in Mendelian populations. Genetics. 16:97–159.

Wright S. 1932. The roles of mutation, inbreeding, crossbreeding and selection in evolution. Proc. 6th Int. Congr. Genet. 1:356–366.

Zachos J., Pagani M., Sloan L., Thomas E., Billups K. 2001. Trends, rhythms, and aberrations in global climate 65 Ma to present. Science. 292:686–693.